AD-A160 004 NONLINEAR PARAMETRIC WAVE MODEL COMPARED WITH FIELD DATA(U) NAVAL POSTGRADUATE SCHOOL MONTEREY CA J L MELO JUN 85 1/1

UNCLASSIFIED F/G 8/3 NL

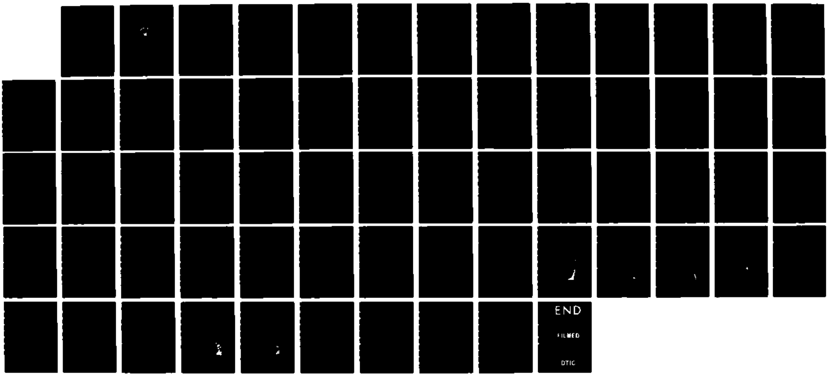

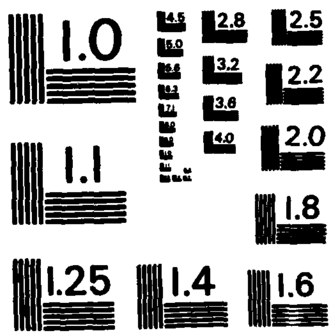
1.0
1.1
1.25
1.4
1.6
1.8
2.0
2.2
2.5
2.8
3.2
3.6
4.0
4.5
5.0

2

NAVAL POSTGRADUATE SCHOOL

Monterey, California

THESIS

NONLINEAR PARAMETRIC WAVE MODEL
COMPARED WITH FIELD DATA

by

Jose Luis Branco Seabra de Melo

June 1985

Thesis Advisor: E.B. Thornton

Approved for public release; distribution unlimited

UNCLASSIFIED

SECURITY CLASSIFICATION OF THIS PAGE (When Data Entered)

REPORT DOCUMENTATION PAGE

READ INSTRUCTIONS BEFORE COMPLETING FORM

1. REPORT NUMBER	2. GOVT ACCESSION NO. AD-A160004
3. RECIPIENT'S CATALOG NUMBER	
4. TITLE (and Subtitle) Nonlinear Parametric Wave Model Compared with Field Data	5. TYPE OF REPORT & PERIOD COVERED Master's thesis June 1985
	6. PERFORMING ORG. REPORT NUMBER
7. AUTHOR(s) Jose Luis Branco Seabra de Melo	8. CONTRACT OR GRANT NUMBER(s)
9. PERFORMING ORGANIZATION NAME AND ADDRESS Naval Postgraduate School Monterey, California 93943-5100	10. PROGRAM ELEMENT, PROJECT, TASK AREA & WORK UNIT NUMBERS
11. CONTROLLING OFFICE NAME AND ADDRESS Naval Postgraduate School Monterey, California 93943-5100	12. REPORT DATE June 1985
	13. NUMBER OF PAGES 62
14. MONITORING AGENCY NAME & ADDRESS (if different from Controlling Office)	15. SECURITY CLASS. (of this report) Unclassified
	15a. DECLASSIFICATION/DOWNGRADING SCHEDULE

16. DISTRIBUTION STATEMENT (of this Report)

Approved for public release; distribution unlimited.

17. DISTRIBUTION STATEMENT (of the abstract entered in Block 20, if different from Report)

18. SUPPLEMENTARY NOTES

19. KEY WORDS (Continue on reverse side if necessary and identify by block number)

Nonlinear Waves, Shallow Water Waves, Spectral Analysis, (Theses) Waves

20. ABSTRACT (Continue on reverse side if necessary and identify by block number)

Wave spectra calculated using the Parameterized Nonlinear Wave Solution developed by Le Mehaute et al. (1984) are compared with field data acquired at Leadbetter beach, Santa Barbara, California. The parameterized solution satisfies the nonlinear free surface boundary conditions to a specified degree of accuracy and is expressed in terms of a converging truncated Fourier series. The wavenumber, surface profile and wave orbital velocities are determined by the wave height and wave period at the local depth of water. Spectral

DD FORM 1473, 1 JAN 73 EDITION OF 1 NOV 65 IS OBSOLETE

S/N 0102-LF-014-6601

UNCLASSIFIED

SECURITY CLASSIFICATION OF THIS PAGE (When Data Entered)

components are compared between the model results and field data. Good agreement is observed for waves corresponding to Ursell numbers ranging from 25 to 75. For large Ursell numbers (strong nonlinear effects) the parameterized model underestimates the data.

Nonlinear Parametric Wave Model Compared With Field Data

by

Jose Luis Branco Seabra de Melo
Lieutenant, Portuguese Navy
Portuguese Naval Academy, 1979

Submitted in partial fulfillement of the requirements for the degree of

MASTER OF SCIENCE IN OCEANOGRAPHY

from the

NAVAL POSTGRADUATE SCHOOL
June 1985

Author: ______________________________
Jose Luis Branco Seabra de Melo

Approved by: ______________________________
Edward B. Thornton, Thesis Advisor

____
Chung-Shang Wu, Second Reader

____
C.N.K. Mooers, Chairman
Department of Oceanography

____
John Dyer,
Dean of Science and Engineering

ABSTRACT

Wave spectra calculated using the Parameterized Nonlinear Wave Solution developed by Le Mehaute et al. (1984) are compared with field data acquired at Leadbetter beach, Santa Barbara, California. The parameterized solution satisfies the nonlinear free surface boundary conditions to a specified degree of accuracy and is expressed in terms of a converging truncated Fourier series. The wavenumber, surface profile and wave orbital velocities are determined by the wave height and wave period at the local depth of water. Spectral components are compared between the model results and field data. Good agreement is observed for waves corresponding to Ursell numbers ranging from 25 to 75. For large Ursell numbers (strong nonlinear effects) the parameterized model underestimates the data.

Keywords: to

TABLE OF CONTENTS

LIST OF TABLES

LIST OF FIGURES

LIST OF SYMBOLS

An	=	Coefficient of parameterized solution
a	=	Wave amplitude
Be	=	Bernoulli constant
c	=	Wave celerity (phase velocity)
d	=	Local depth below still water level
e_1	=	Individual dynamic boundary condition error
e_2	=	Individual kinematic boundary condition error
E_1	=	Root mean square of e_1
E_2	=	Root mean square of e_2
E_3	=	Error of wave crest-wave trough distance to input wave height
g	=	Acceleration of gravity
H	=	Wave height
K	=	Integration constant
k	=	Nonlinear wave number
k*	=	Linear wave number
Lo	=	Linear wavelength in deep water
L*	=	Linear wavelength
N	=	Number of terms in Fourier series expression
T	=	Wave period
z	=	Measurement elevation
γ	=	Wave steepness
δ	=	Relative water depth
ϵ	=	Wave steepness (ak)
η	=	Water wave surface elevation
θ	=	Phase angle
σ	=	Wave angular frequency
Φ	=	Dimensionless velocity potential
ϕ	=	Velocity potential.

ACKNOWLEDGEMENTS

Living at a time in which costs of instruction still need to be paid, the author wishes to express his thanks to his PARENTS for their sacrifices and support for him to reach his present educational level.

The author is gratefully indebted to Dr. Edward B. Thornton, Professor of Oceanography at the Naval Postgraduate School, Monterey, California, as thesis advisor, for his strong support and orientation in the preparation of this study. Thanks go to Dr. Chung-Shang Wu, who offered helpful suggestions and encouragement. The assistance of Ms. Donna M. Burych is also gratefully acknowledged.

Lastly, and most importantly, I wish to thank my wife, Paula, for her patience, understanding and encouragement and for her editing of my English in the thesis.

I. INTRODUCTION

The random nature of ocean waves is most often described using the linear spectral model, and many engineering problems related to offshore and coastal structures are solved by employing the concept of directional wave spectra. Waves in the sea, however, can exhibit nonlinear properties. A departure of surface elevation from the Gaussian distribution with positive skewness is an example. Phase velocities of high frequency component waves not satisfying the linear dispersion relation is another example. Breaking of waves is a spectacular example of nonlinear behaviour of water waves.

The study of nonlinear, water waves traveling over a horizontal bottom dates back to Stokes(1847), who solved this problem in the form of a power series in terms of a small parameter 'ϵ' related to the average wave slope (ϵ = ak, where a is the wave amplitude and k is the wavenumber). It was found, however, that the Stokesian type series are nonuniformly convergent, and are only valid in deep and intermediate water depth.

Boussinesq (1877) and Korteweg and de Vries (1895) developed the cnoidal wave theories, which are based upon power series in terms of wave height relative to water depth. These power series are uniformly convergent in shallow water, but are invalid in deep water.

Making the connection between the two above theories, Goda (1983) developed an empirical parameter to describe the phenomena of wave nonlinearities with good results. The parameter bridges the wave steepness in deep water and the Ursell's parameter $Ur = (a/d)/(d/L)^2$ (with a the wave amplitude, d the water depth, and L the local wave length) in very shallow water, spanning the full range of water waves.

When confronted with experimental results, Le Mehaute et al. (1968) demonstrated that the nonlinear theories were not much better than the linear wave theory; nonetheless there is a need to clarify the extent of wave nonlinearity in the sea so that engineering problems can be solved with much more confidence and accuracy.

During the last two decades, numerical approaches based on truncated Fourier expansions have been proposed and well verified experimentally. The first such approach was developed by Chappelear (1961) involving the use of the velocity potential. Dean (1965) used the stream function to develop his numerical wave theory, which was computationally simpler than Chappelear's technique. Dean's stream function form satisfies the Laplace equation, the kinematic free surface boundary condition, and the bottom boundary condition; the parameters in the stream function expression are chosen by a best fit to the dynamic free surface boundary condition. Von Schwind and Reid (1972) developed characteristic solutions to finite amplitude waves using the velocity potential. Cokelet (1977) extended the method originally developed by Schwartz (1974) to allow a very accurate calculation of the characteristics of water waves. The procedure involves expressing the complex potential solution in a Fourier series and represents the Fourier coefficients in terms of a perturbation parameter. Rienecker and Fenton (1980) used a finite Fourier series to describe waves by solving a set of nonlinear equations using Newton's method. Recently, Le Mehaute et al. (1984) developed a parameterized solution which is valid for all practical ranges of values of wave amplitude, frequency and water depth. In view of its relative simplicity, and experimental validity, the parameterized solution is recommended for engineering applications.

The objective of this work is to utilize the spectral model by Le Mehaute et al. (1984) to compare with wave data acquired at Santa Barbara during the 2-6 February, 1980. The range of application of the model will be checked against measured wave spectral components and individual waves. The wave nonlinearity and Ursell number are analyzed using the model. Comments and conclusions are made for further study.

II. THEORETICAL BACKGROUND

A. PARAMETERIZED SOLUTION TO THE NONLINEAR WAVE PROBLEM

1. Overview

The higher-order Stokian wave theories become algebraically very complex. For practical purpose, it was desirable to develop wave theories that could be computed to any order. Le Mehaute et al. (1984) developed a parameterized solution to the monochromatic, irrotational, nonlinear water wave over a horizontal bottom. The formulation is expressed in a closed form in terms of a truncated Fourier series. All coefficients are expressed in terms of simple analytical functions which contain three parameters, namely, wave height, H, wave period, T, and water depth, d. The number of terms in the Fourier series is proposed parametrically for a given level of accuracy. The solution is assumed to be applicable for all practical ranges from deep to shallow water waves, i.e., $d/Lo \geq 0.005$. The deep water solution for $d/Lo = 0.5$ is assumed to be valid for $d/Lo > 0.5$.

2. Theoretical Formulation

As in the periodic water wave problem the formulation has linear and nonlinear boundary conditions and a linear governing differential equation.

Choosing a coordinate system moving with wave speed $c = \sigma / k$ so that the time dependency is removed, i.e., a stationary problem , it is possible to assign a constant value to the stream function at the free surface. The variable σ is the wave angular frquency ($\sigma = 2\pi/T$) and k is the wavenumber ($k = 2\pi / L$). The solution is a velocity potential function of the form

$\phi\{(x-ct),z\}$ or $\phi(\theta,z)$ which satisfies the Laplace equation :

$$\nabla^2\phi = 0 \tag{2.1}$$

The variable $\theta = kx - \sigma t$ denotes phase, and the z axis is vertical positive upwards from the S.W.L. (still water level) and the horizontal x axis is positive in the direction of wave propagation.

The kinematic bottom boundary condition is written as

$$\phi_z \big|_{z=-d} = 0 \tag{2.2}$$

The dynamic free surface boundary condition, is derived using Bernoulli's equation written in the dimensionless form at $z = \eta$

$$\frac{1}{H}\left\{\eta + \frac{1}{2g}\left[\left(\phi_x - c\right)^2 + \phi_z^2\right] - \frac{c^2}{2g} - B_e\right\} = e_1(\theta) \tag{2.3}$$

where H is the wave height, η is the water wave surface elevation and Be = an arbitrary Bernoulli constant.

The kinematic free surface boundary condition is

$$\eta_x - \frac{\phi_z}{\phi_x - c} = e_2(\theta) \tag{2.4}$$

The e's are the allowable errors which should be small.

The measure of how well these two boundary conditions are satisfied is defined by E_1 , and E_2, which are the mean squared errors of the dynamic and kinematic free surface boundary conditions :

$$E_1=\left[\frac{1}{J}\sum_{j=1}^{J} e_{1j}^2(\theta)\right]^{1/2} \tag{2.5}$$

$$E_2=\left[\frac{1}{J}\sum_{j=1}^{J} e_{2j}^2(\theta)\right]^{1/2} \tag{2.6}$$

in which j = sample at evenly spaced phase angles (e.g., with 5° interval) along the wave profile. The Bernoulli constant, Be, is determined such that the variation cf the phase speed c is minimized over a wavelength. For an exact solution, E_1 and E_2 would be zero.

A solution in the form of a limited series (or truncated Fourier expansion) is assumed

$$\Phi = \frac{\phi\,\sigma}{a\,g} = \sum_{n=1}^{N} A_n \cosh\left[nk(d+z)\right]\sin n\theta \tag{2.7}$$

in which Φ = dimensionless potential function; An = a derived coefficient; n is an integer and N = the number of terms. All the internal wave field terms (velocity components, dynamic pressure and acceleration components) can be directly determined from this equation. Eq. 2.7 satisfies both the Laplace equation (2.1) and the kinematic bottom boundary condition (2.2) exactly.

The equation for the free surface correponding to eq. 2.7 is:

$$\frac{\eta}{2a} = \frac{K}{2a} - \frac{gk}{2\sigma^2}\sum_{n=1}^{N} A_n \sinh\left[nk(d+\eta)\right]\cos n\theta \tag{2.8}$$

in which K = an integration constant satisfying

$$\int_0^{\pi} \eta\, d\theta = 0 \tag{2.9}$$

At the wave crest (θ = 0), $\eta = \eta_c$ and the wave trough ($\theta = \pi$), $\eta = \eta_t$ .Therefore

$$\frac{\eta_c + |\eta_t|}{2a} = 1 + E_3 \qquad (2.10)$$

in which E_3 is to be determined and must be small.

Le Mehaute et al (1984) defines the phase velocity c or wavenumber k in accordance with the Hamiltonian variational principle of minimum energy, which, in practice, is obtained through minimizing E_1 with respect to the wavenumber, k

$$\frac{\partial E_1}{\partial k} = 0 \qquad (2.11)$$

Such a system of equations can eventually be solved as a function of phase velocity.

The solution to the problem consists in providing an analytical solution which describes all the wave characteristics as functions of only three parameters : wave height, H, wave period, T, and water depth, d. These parameters are grouped into two dimensionless parameters

Depth parameter: $$\delta = \frac{d}{L_o} = \frac{d\sigma^2}{2\pi g} \qquad (2.12)$$

Wave steepness parameter: $$\gamma = \frac{H}{L_o} = \frac{a\sigma^2}{\pi g} \qquad (2.13)$$

in which Lo is the linear deep water wavelength and a = H/2 is the wave amplitude.

Having specified the initial boundary value problem and analytical forms of eqs. 2.3 and 2.4, the problem now consists of expressing all unknowns ; An, k, K, and N (eq. 2.8), in terms of the two parameters δ and γ , such that a desired level of accuracy is achieved. These unknowns are determined by satisfying the boundary criteria as closely as possible. Eq. 2.11, which specifies the phase velocity and wave number, must also be satisfied. The method of solution is one of trial and error involving multiple iterative processes as expressed in the flow chart in Figure 1.

For practical purposes, the final formulation may be presented in the following:

INPUT DATA : Given H, T, and d then

$$L_o = gT^2/2\pi, \quad k^* = 2\pi/L^*, \quad k = 2\pi/L, \quad \sigma = 2\pi/T$$

$$\delta = d/L_o \quad \text{and} \quad \gamma = H/L_o \quad \text{. Also,} \quad \beta = \gamma/\tanh(4.588\delta^{0.995})$$

$$\text{and} \quad \sigma^2 = g k^* \tanh k^* d \, .$$

(The symbol * denotes the linear solution).

FORM OF SOLUTIONS:

$$\phi = \frac{a g}{\sigma} \sum_{n=1}^{N} A_n \cosh\left[n k \left(d + z\right)\right] \sin n\theta \qquad (2.14)$$

$$\eta = K - \frac{a g k}{\sigma^2} \sum_{n=1}^{N} A_n \sinh\left[n k \left(d + \eta\right)\right] \cos n\theta \qquad (2.15)$$

INTEGRATION CONSTANT: For application purposes, a parameterized form of K is determined by

$$K = -1.764 \frac{a\, g\, k}{\sigma^2} \beta^{0.55} \delta^{0.77} \qquad (2.16)$$

The use of K as expressed above generally yields larger values of E's than the value of K obtained by eq. 2.9 directly.

NONLINEAR WAVE NUMBER : $k = 2\pi/L$

1. $0.005 \leq \delta \leq 0.1$

$$k = k' = \frac{k^*}{\left[1 + 1.879\beta^{1.097} - 0.094\beta^{0.528} \ln(2 \times 10^2 \delta)\right]} \qquad (2.17)$$

2. $0.1 < \delta \leq 0.5$

$$k = k'' = \frac{k^*}{\left[1 + \frac{3.466}{\tanh k^* d} \beta^{1.5} \delta^{0.315}\right]} \qquad (2.18)$$

The solution valid for $\delta = 0.5$ is also considered valid for $\delta > 0.5$ provided that all the parameterized functions which follow are determined with $\delta = 0.5$ irrespective of their real value; this means that deep water solutions corresponding to $\delta > 0.5$ are not influenced by water depth.

COEFFICIENTS:

<u>Coefficient A_1</u>:

$$A_1 = A^*(1 - R) \qquad (2.19)$$

$$A^* = -\frac{1}{\cosh k^* d} \tag{2.20}$$

1. $0.005 \leq \delta \leq 0.1$

$$R = a_1' (5.882\beta)^{b_1'} \tag{2.21}$$

in which $a_1' = 0.8132 \exp\{-0.0153 [\ln(10^3 \delta)]^{2.82}\}$

$b_1' = 0.0747 \exp\{1.1057 [\ln(10^3 \delta)]^{0.75}\}$

2. $0.1 < \delta \leq 0.5$

$$R = 0.3 + (-0.3 + a_1'') \exp\left\{ b_1'' [\ln(10\delta)]^{c_1''} \right\} \tag{2.22}$$

in which $a_1'' = 17.30\beta^{2.38}$

$b_1'' = 1.389 \tanh^{-1}(24.09\beta^{1.836})$

$c_1'' = 1.3676 \exp(-179.0\beta^{3.04})$

<u>Coefficient A_2</u> :

1. $0.005 \leq \delta \leq 0.1$

$$A_2 = 0.497 A_1 \exp\left[a_2' (5.882\beta)^{b_2'}\right] \tag{2.23}$$

in which $a_2' = -0.00933 \exp\{1.494 [\ln(10^3 \delta)]^{0.79}\}$

$b_2' = -0.953 \exp\{-0.029 [\ln(10^3 \delta)]^{2.01}\}$

2. $0.1 < \delta \leq 0.5$

$$A_2 = 2.5 \times 10^{-5} A_1 \exp\left[a_2'' \exp(b_2'' \delta^{c_2''})\right] \tag{2.24}$$

in which $a_2'' = 10.547 \exp(-0.0134\beta^{-0.98})$

$$b''_2 = -16+15.318 \exp(-0.0017\beta^{-1.78})$$

$$c''_2 = 5-4.328 \exp(-0.0112\beta^{-1.04})$$

<u>Coefficient A_3</u> :

1. $0.005 \leqslant \delta \leqslant 0.1$

$$A_3 = 0.672\, A_2 \exp\left[a'_3\, (5.882\beta)^{b'_3}\right] \tag{2.25}$$

in which $a'_3 = -0.021 \exp\{1.355 \left[\ln(10^3\, \delta)\right]^{0.78}\}$

$b'_3 = -0.859 \exp\{-0.0747 \left[\ln(10^3\, \delta)\right]^{1.28}\}$

2. $0.1 < \delta \leqslant 0.5$

$$A_3 = A_2 \exp(a''_3) \tag{2.26}$$

in which $a''_3 = -3.537\,\delta^{0.52}\beta^{-0.418}$

<u>Coefficient An</u> ($n > 3$)

$$A_n = A_{n-1} \exp(-3.537\,\delta^{0.52}\beta^{-0.418}) \tag{2.27}$$

3. <u>Analytical Validity</u>

The validity of this theory is defined through the E values as derived by eqs. 2.3, 2.4, 2.5, 2.6, 2.10 and 2.11 by order of importance. The magnitude of the E's depends on the number of terms N used in the series. Beyond a certain value of N, it is found that the E values tend towards asymptotic values, indicating that they are not reduced by adding more terms, i.e., the series is bounded. With this property in the solutions, the number of terms N required can be expressed in parameterized form by :

$$N = \text{integer part of}\{n_1 + n_2(5.38\ \beta - 0.2)\} \quad (2.28)$$

$$n_1 = 1 + 19.13 \exp\{-0.344 [\ln(10^3\ \delta)]^{(1.12)}\} \quad (2.29)$$

$$n_2 = 32.72 \exp\{-0.212 [\ln(10^3\ \delta)]^{(1.31)}\} \quad (2.30)$$

Le Mehaute et al, (1984) showed that the parameterized solution approximates the free surface dynamic boundary condition as well as, if not better, than any other existing theory. It also approximates the kinematic condition generally better, except for the stream function theory developed by Dean (1974) by virtue of its definition.

Truncated Fourier series do not represent limit waves well since the cusp at the wave crest requires an infinite number of terms as was demonstrated by Dean (1974). Therefore, the accuracy of the parametric solution decreases rapidly as the wave heights approach limit wave conditions, which is where Ur is large.

B. MEASURE OF NONLINEARITY

The parameter which represents the wave nonlinearity in deep water is the wave steepness, or a measure of the surface elevation slope. The most common representation is either the ratio of wave height to wavelength H/L, or the parameter ak.

In the region of shallow water waves, the Stokian wave profile for higher orders is an expansion using the nondimensional term

$$Ur = (a/d)/(d^2/L^2) \quad (2.31)$$

as the perturbation parameter. This term is called the Ursell parameter and has been shown to govern the transformation of water waves in shallow water. For example, it has been demonstrated that the nonlinear shoaling of water waves is predicted as the function of the Ursell's parameter.

When Ur << 1, the linear small amplitude wave theory applies. In principle, more and more terms of the power series are required in order to keep the same relative accuracy as the Ursell parameter increases.

The Ursell parameter is a usefull guide, but is not necessarily sufficient for judging the relative importance of the nonlinear effects. A qualitative idea of the importance of nonlinearity is also given by the ratio of spectral values of each harmonic frequency to the spectral value of the fundamental frequency. However, the nonlinear effects of shoaling transformation are cumulative, so that the nonlinearities may be locally weak, but significant cross-spectral transfer can occur if the shoaling region is wide in comparison to the nonlinear interaction distance.

III. EXPERIMENTAL PROCEDURES

Wave and velocity data acquired at Santa Barbara, California, during the 2nd, 3rd, 4th, 5th and 6th February 1980, as part of the Nearshore Sediment Transport Study, are used to be compare with the parameterized model. The field data, considered in this work, include only measurements made by the current meters outside the breaking zone. Current meters C07X, C03X and C01X (see Figure 2) are used on the 2nd and 6th of February; current meters C03X, C01X and C0DX are used on the 3rd of February, and C01X and C0DX are used on the 4th of February.

For each day and each instrument the following statistics were calculated: average wave height, $\bar{H}$, the maximum wave height, Hmax, the significant wave height, H1/3, the root mean squared wave height, Hrms, and the average of the heights of the 1/10 highest waves, H1/10, as well as the associated water depths, and the surface elevation spectrum.

A. WAVE SPECTRAL ANALYSIS

The surface elevation spectra were calculated from 68 minute current meter records. The water particle velocity components measured by the current meters were recorded on a special receiver/tape recorder, digitally low-pass filtered and sampled at 2 samples/sec. The data were then high-pass filtered at 0.05 hz to exclude low frequency variations. These current data were used to infer wave heights. The velocity signals were convolved using linear wave theory to obtain surface elevations. The complex Fourier spectra of the horizontal velocity components were first calculated and vectorially added to give $V(f)$. The complex surface elevation spectrum, $X(f)$, was calculated applying the linear wave theory transfer function $H(f)$

$$X(f) = H(f) * V(f) \tag{3.1}$$

where

$$H(f) = (\sinh kd)/\{\sigma \cosh k(d+z)\} \tag{3.2}$$

with z = measurement of elevation.

The calculated energy density spectra are to be compared with the parametric model. Since the parametric model defines all the truncated Fourier series coefficients as simple analytical functions in terms of the wave height H, wave period T, and water depth d, it was necessary to transform the energy density spectra of the sea-surface elevation into a discrete (spikes) spectra as shown in Figure 3.

The discrete spectra were calculated by first finding the fundamental frequency defined as the frequency associated with the highest energy density peak. The harmonics were defined as the integer mutiples of this fundamental frequency. The bandwidths associated with the energy peaks were defined at the frequencies corresponding to the half power points of the energy density values. The variance of the peaks, calculated as the area of the energy density spectrum between half power points, describe the height of the spectral spike. The analysis was carried out to the highest harmonic for which half power points could be defined. The reason for defining the bandwidths at the half power points is because the half power values correspond to the level at which the spectral components are independent of one another. It was noted that the bandwidth increases approximately with the number of harmonic.

Assuming $\overline{\eta} = 0$, the variance of the wave surface is given by

$$\text{var} = \frac{1}{T}\int_T \eta^2 dt \qquad (3.3)$$

The parameterized variance, or energy, can be defined from equation 2.15 in the discrete mode

$$\text{var}(n) = K^2 + \frac{1}{2}\left(\frac{a g k}{\sigma^2}\right)^2 \left\{ A_n \sinh\left[nk\left(d+\eta\right)\right]\right\}^2 \qquad (3.4)$$

with n = 1,2,3...N.

The wave height (and wave amplitude) used to calculate the parametric energy line spectrum was the average wave height, $\overline{H}$, because it was the wave height parameter which offered best fitting to the field data.

Comparisons for all days were made between the converted actual line spectrum and the parametric line spectrum calculated using the input parameters of average wave height $\overline{H}$, average water depth d, and the period corresponding to the defined fundamental frequency (T = 1/f), calculated for the 68 minute measurements.

B. INDIVIDUAL WAVE ANALYSIS

A second approach was to compare individual waves measured in the field with the parametric model predictions. The filtered and digitized velocity signals were convolved using linear theory to obtain surface elevations. The individual waves were defined using the zero-up crossing method as explained in Figure 10. The highest maximum and the lowest minimum of the surface elevation within a period interval define the crest and the trough of a wave. A wave height Hi is defined as the range of η (t) in that interval, the period is the time interval between two consecutive zero-up crossings of η (t).

A Fourier analysis was performed on each individual wave using a Fast Fourier Transform algorithm. The parametric coefficients associated with the surface elevation formula were also determined for each wave using the measured Hi, Ti, and di. Statistics of Fourier coefficients from field data and the parametric model were generated for each day

$$\overline{An} = (1/Nw) * \sum_{i=1}^{Nw} An(i) \qquad (3.5)$$

(where Nw = number of analyzed waves). For each run comparisons were made between this approach and the wave spectral analysis. Since the average wave period was about 15 seconds, the total number of waves in each 68 minutes record was about 300, which give reasonable wave statistics.

C. SUMMARY

Both analyses were based on the similarity between the Fourier series representation of the sea surface elevation

$$\eta(t) = a0 + \sum_{n=1}^{\infty} an \cos n\theta \qquad (3.6)$$

(with a0 = mean) and the sea surface elevation described by the parametric model as defined by the equation 2.15. The coefficients to be compared are the an's for the Fourier series defined by the Fourier integrals and the Le Mehaute coefficients

$- (1/\sigma**2) *a*g*k* An * \sinh\{nk(d+\eta)\}$

where An are defined parametrically as function of the depth parameter δ and wave steepness γ, and η defined iteratively from equation 2.15.

The spectral data analysis is a linear approach. The spectral components are assumed independent of each other. The analysis considers that the spectral component phase angles at each frequency are random (putting the problem in a probabilistic or stochastic setting). On the other hand, the individual wave analysis is also a linear approach, but the phase relationship between harmonics is presumed deterministic (i.e. phase coupled with the fundamental frequency, as evidenced by the observed peaked crests and flattened troughs).

IV. RESULTS

A. SPECTRAL ANALYSIS

1. Nonlinear Statistics

A typical energy density spectrum for all analyzed instruments is presented in Figure 2 (upper panel). The presence of strong harmonics in the spectrum indicates the importance of nonlinearities of the waves in this region of shallow water. A qualitative idea of the importance of nonlinearity is given by the ratio of the harmonic energies to the primary frequency energy $E(nf)/E(f)$, where $n = 2, 3 \dots$ are the harmonic frequencies. Due to the difficulty of defining the half power points for the harmonics higher than the third, only the ratios involving the first and second harmonics are presented.

Tables I - V give the ratios for all five days studied for both the parameterized model (denoted L.M.) and the field data (denoted by F.).The water depth and the Ursell parameter associated with each measurement are also presented. The range of water depths is from about 670 cm to 138 cm. The range of the Ursell parameter is from about 6 to 120.

For large Ursell numbers ($Ur > 75$), the parameterized model overestimates the importance of the energy associated with the harmonics relatively to the fundamental frequency energy. The same ratios for the field data are 20 - 60 percent lower. For small Ursell numbers ($Ur < 25$), the parameterized model underestimates the importance of the harmonics relatively to the fundamental frequency energy. The same ratios for the field data are 0.5 - 40 percent higher.

The best fitting between the parameterized model and the field data occurs at intermediate Ursell numbers (25 < Ur < 75). It is found that the parameterized model energy ratios compared with the field data energy ratios have an error of less than 20 percent for the cases of intermediate Ursell number. Some exceptions were observed to the above indicated percentages, but the energy contribution at these frequencies is very small.

2. Local Spectral Comparisons

An absolute comparison was made between the parameterized model spectral energy peaks and field data spectral energy peaks as a function of frequency. Typical results for three different Ursell numbers are presented in Figures 4 and 5. In regions of strong nonlinear effects (large Ursell number), the parameterized model underestimates the energy at the fundamental frequency. The energy drops linearly from the fundamental frequency to the harmonics, in the parameterized model, while field data spectra fall off much faster. In regions of small Ursell numbers the parameterized model concentrates almost all the energy in the fundamental frquency, overestimating it relative to the field data. The best agreement between the parameterized spectral energy peaks and field data energy peaks are observed for intermediate Ursell numbers.

The Fourier coefficients used to evaluate field data spectra are plotted against the Le Mehaute spectral coefficients (1 / σ **2) agkA sinh{nk(d + η)} (Figs. 6-8). A reasonable correlation is found for the first three coefficients.

The spectral analysis approach is summarized by plotting the ratio of the Le Mehaute spectral peaks to field data spectral peaks against the Ursell parameter (Fig. 9). The ratio for the fundamental frequency energy decreases as the Ursell parameter increases emphasizing how the parameterized model underestimates the fundamental frequency spectral peak in situations of strong nonlinearities (large Ursell parameter). The ratios for both the first and second harmonic frequency energies increase as the Ursell parameter increases; it must be noted, as indicated earlier, that the data only ranges in Ursell numbers from about 6 to 120.

B. INDIVIDUAL WAVE ANALYSIS

Individual waves were identified using the zero-up-cross method. A Fourier analysis was performed on each individual wave. The parameterized spectral coefficients were also determined for each individual wave.

The Fourier coefficients associated with the fundamental frequency, first and second harmonics are plotted separately against the corresponding parameterized coefficients. The coefficients at the fundamental frequency (Fig. 14) are reasonably well correlated (correlation coefficient = 0.80). The Fourier coefficients plotted against the Le Mehaute coefficients follow a straight line with intercept at the origin and slope of about one. The group of plotted points with a greater slope (approximately 2) are associated with measurements in shallower waters with higher Ursell numbers (see Figs. 12-16). The graphs of the the first and second harmonic coefficients (Figs. 17-18) show similar characteristics as the fundamental frequency; however, the correlation between the coefficients is poorer.

The ratio of the Le Mehaute coefficients to the Fourier coefficients is also plotted against the Ursell parameter The ratio for the fundamental frequency coefficients converge to a bound value of 0.5 at large Ursell numbers (Fig. 19). For Ursell numbers less than 75 the ratio of the Le Mehaute to Fourier coefficients is about 1 with the exception of a few points near Ur = 0 which were identified to be related with noisy signals. For large Ursell numbers the Fourier coefficients are about twice the Le Mehaute coefficients, again showing the tendency that the parameterized model has to underestimate the fundamental peak energy in regions of strong nonlinearities (large Ursell numbers).

The ratios for the first and second harmonic coefficients (Figs. 19 and 20) show a bounded value near unity as the ursell parameter increases. Noisy signals near Ur = 0 are also observed.

C. COMPARISONS BETWEEN APPROACHES

Both linear (spectral analysis) and nonlinear (individual wave analysis) approaches lead to similar results. The parameterized model is observed to overestimate the fundamental frequency energy in regions of small Ursell number (weak nonlinearities) and underestimate it in regions of large Ursell number. The individual wave analysis presents a limit tendency for large Ursell numbers, with the fundamental frequency Fourier coefficients about twice those of the parameterized spectral coefficients. The better correlation observed between the Fourier coefficients and the Le Mehaute coefficients in the individual wave analysis as compared with spectral analysis approach is due, perhaps, to the definition of half-power criteria or to the averaging processes involved in calculating the wave spectra.

The reason for the similarity of results for the two approaches can be seen by comparing the spectra calculated in the usual manner with a "nonlinear spectrum". A nonlinear spectrum was calculated using the Fourier amplitude coefficients calculated for the individual waves. Using the same bandwidths as the ordinary spectrum, amplitude coefficients were sorted into the respective frequency bands and a nonlinear spectrum calculated as

$$Gnl\ (f) = (1/Nw) \sum_{i=1}^{N_w} A_i^2(f)\ /\ 2\Delta f \qquad (4.1)$$

where the coefficients Ai(f) are centered on frequency f within bandwidth Δ f. The total number of waves is denoted by Nw. An example of the comparison of the nonlinear spectrum calculated in this manner with the linear spectral method is shown in Figure 21. The two spectra are similar and both show strong harmonic peaks. The spectral energy in the ordinary spectrum tends to be smeared more, whereas the peaks and valleys in the nonlinear spectrum are more sharply defined.

V. CONCLUSIONS

The coefficients of the parameterized solution to the monochromatic, irrotational, nonlinear wave over a horizontal bottom, as developed by Le Mehaute et al. (1984), are expressed in terms of simple analytical functions of wave height, H, wave period, T,and water depth, d. All quantities explicitly derived from the potential function (velocity components, dynamic pressure, acceleration, i.e., the internal wave field) can be directly determined. The relative simplicity of the calculations of the parameterized solution recommends it for engineering applications.

The wave spectra determined from the parameterized solution show good agreement with the measured wave spectra from field data for conditions of intermediate Ursell numbers (25 < Ur < 75). For small Ursell numbers, the parameterized solution concentrates almost all the energy in the fundamental frequency representing a sinusoidal waveform. Under these conditions, the field wave spectra always contained relatively less energy associated with the fundamental frequency and more energy distributed to the harmonics.

For large Ursell numbers, the parameterized solution describes a waveform with more peaked crests and flatter throughs relative to the measured waves, since it underestimates the energy associated with the fundamental frequency and overestimates the energy associated with the higher harmonics.

The ratios between the Le Mehaute and field data spectral coefficients associated with the 1st and 2nd harmonics present a bound limit tendency of 1 for large Ursell numbers, indicating good agreement between the two processes for these conditions. The same ratios for the coefficients associated with the the fundamental frequency show a bound limit tendency of 0.5, indicating that the first coefficient of the parameterized model needs to be corrected for strong (Ur > 75) nonlinear effects.

Further comparisons should be made for different sea conditions to determine the corrections to the parameterized model coefficients. However, it must be noted that a limitation of the parameterized solution is that its accuracy decreases rapidly as the wave heights approach limiting wave conditions due to the use of a truncated Fourier series.

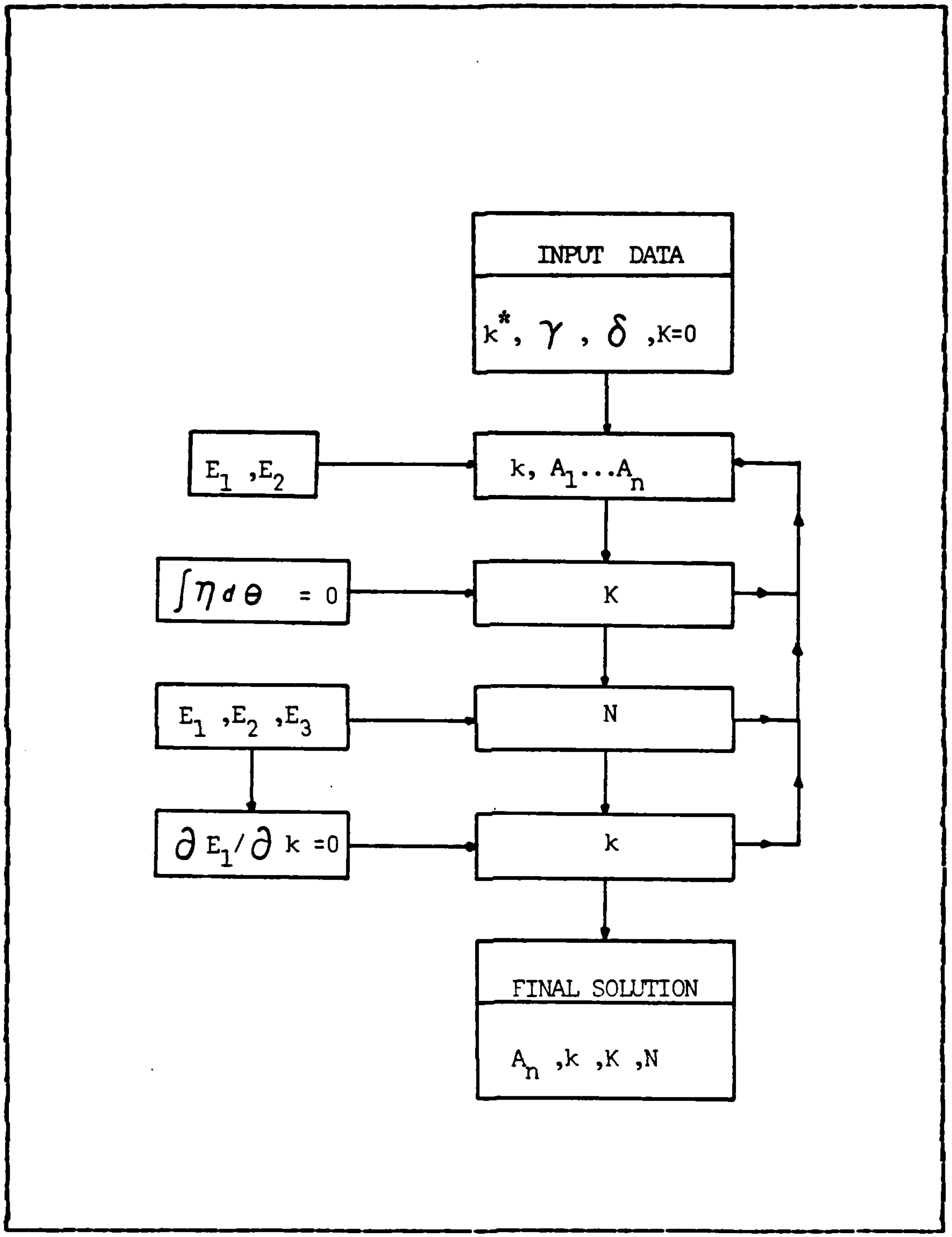

Figure 1 Flow Chart of the Parameterized Nonlinear Wave Model.

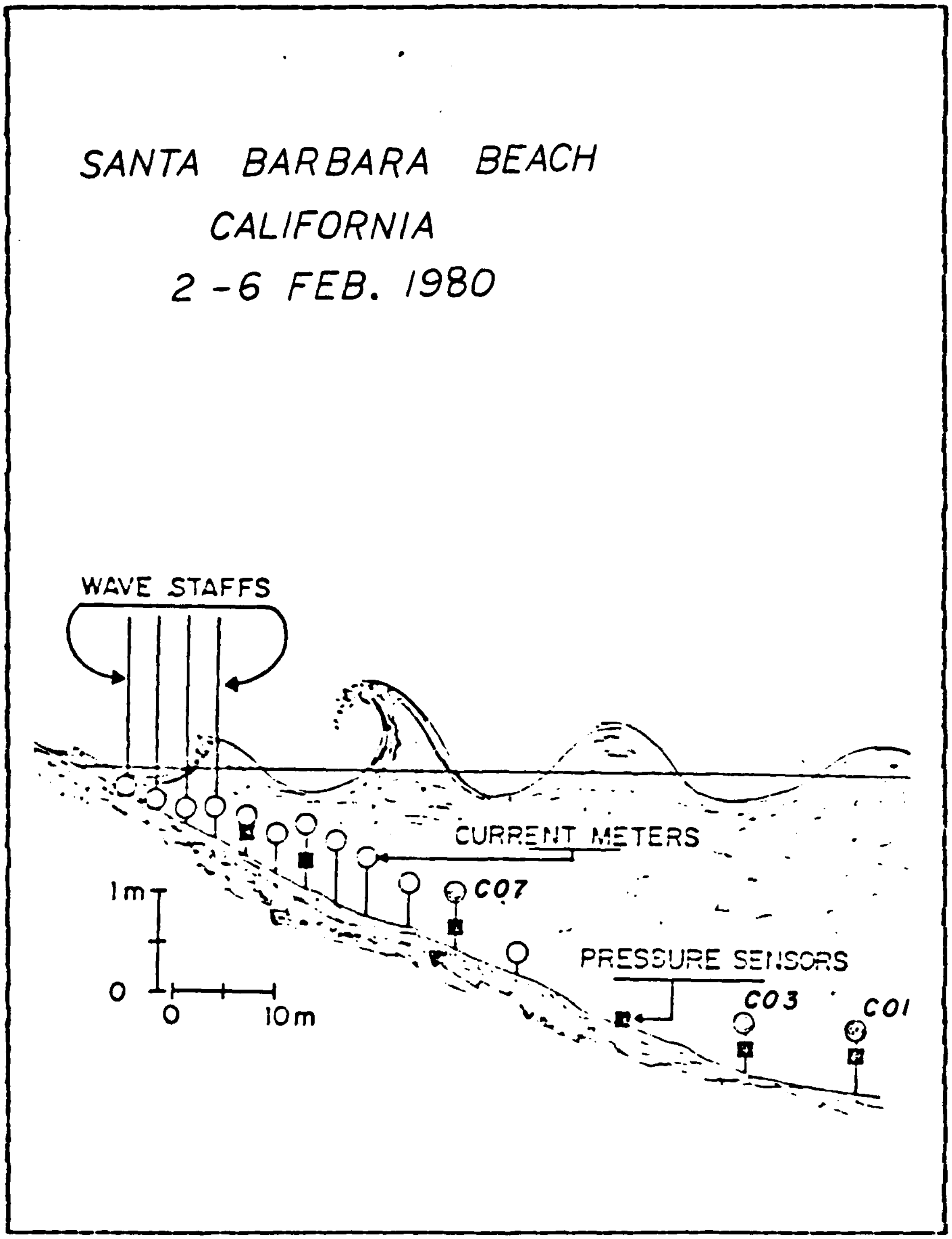

Figure 2 Beach Profile with the Instruments Location.

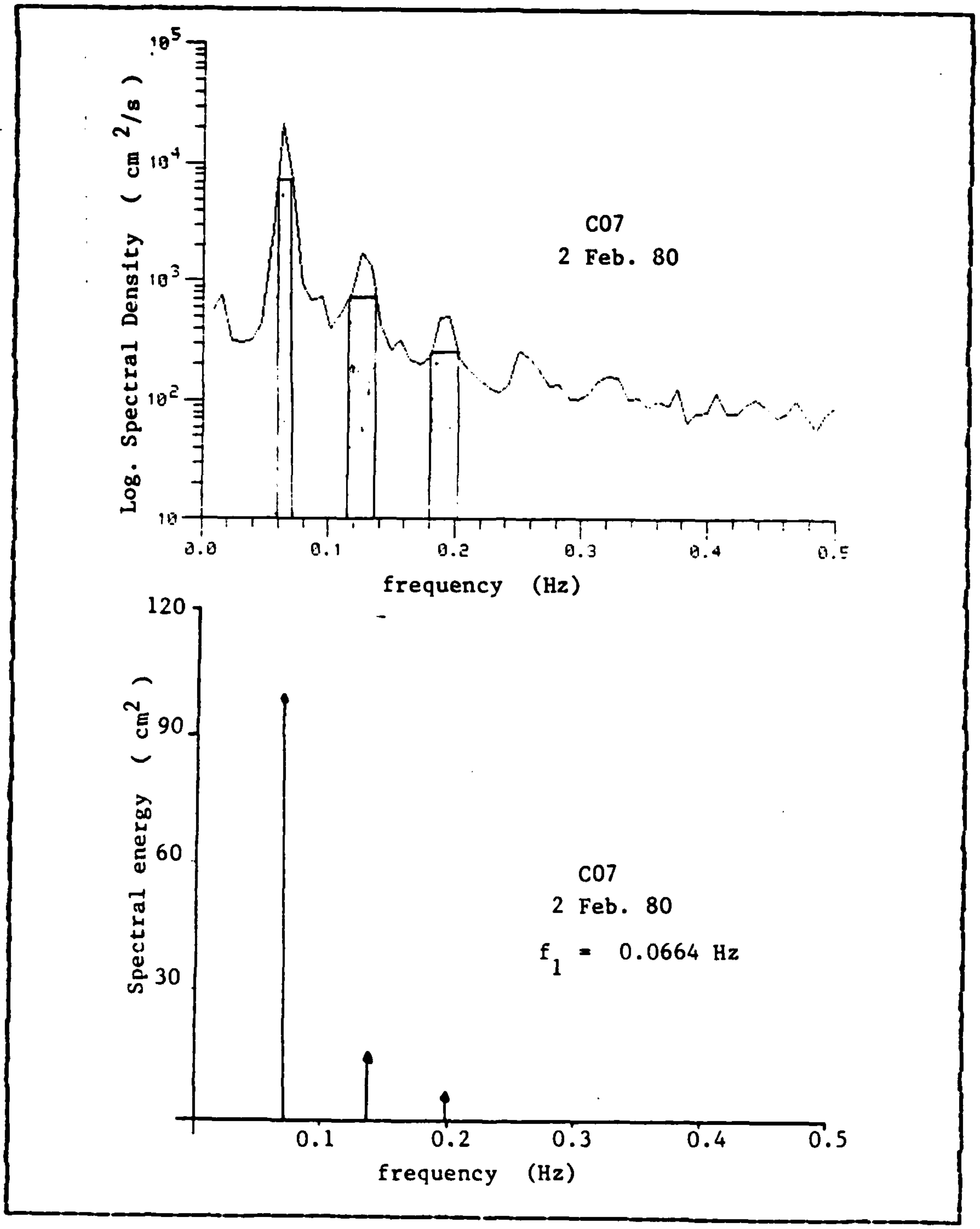

Figure 3 Typical Energy Density Spectrum (above) and Conversion into Discrete Energy Spectrum (below).

TABLE I

Ratio of Harmonic Energy to Primary Frequency Energy
02 FEB. 80

DEPTH (cm)	212.5		333.7		398.7		669.6	
URSELL No.	115.6		31.3		23.4		7.6	
------------	L.M.	F.	L.M.	F.	L.M.	F.	L.M.	F.
E(2f)/E(f)	0.548	0.165	0.167	0.132	0.108	0.120	0.008	0.021
E(3f)/E(f)	0.236	0.056	0.019	0.061	0.008	0.028	-	-
Instrument	C07X		C03X		C01X		CODX	

TABLE II

Ratio of Harmonic Energy to Primary Frequency Energy
03 FEB. 80

DEPTH (cm)	302.3		379.8		650.7	
URSELL No.	63.4		31.7		11.1	
------------	L.M.	F.	L.M.	F.	L.M.	F.
E(2f)/E(f)	0.365	0.194	0.173	0.150	0.025	0.145
E(3f)/E(f)	0.097	0.073	0.021	0.064	0.008	-
Instrument	C03X		C01X		CODX	

TABLE III

Ratio of Harmonic Energy to Primary Frequency Energy
04 FEB. 80

DEPTH (cm)	378.8		649.7	
URSELL No.	31.2		7.9	
------------	L.M.	F.	L.M.	F.
E(2f)/E(f)	0.171	0.159	0.013	0.125
E(3f)/E(f)	0.020	0.054	0.001	0.014
Instrument	C01X		C0DX	

TABLE IV

Ratio of Harmonic Energy to Primary Frequency Energy
05 FEB. 80

DEPTH (cm)	363.6		634.6	
URSELL No.	24.8		6.8	
------------	L.M.	F.	L.M.	F.
E(2f)/E(f)	0.123	0.101	0.008	0.069
E(3f)/E(f)	0.01	0.050	0.001	0.034
Instrument	C01X		C0DX	

TABLE V

Ratio of Harmonic Energy to Primary Frequency Energy
06 FEB. 80

DEPTH (cm)	138.8		278.7		345.4	
URSELL No.	115.5		23.8		11.5	
------------	L.M.	F.	L.M.	F.	L.M.	F.
E(2f)/E(f)	0.548	0.186	0.113	0.196	0.027	0.110
E(3f)/E(f)	0.236	0.068	0.009	0.088	0.002	0.049
Instrument	C07X		C03X		C01X	

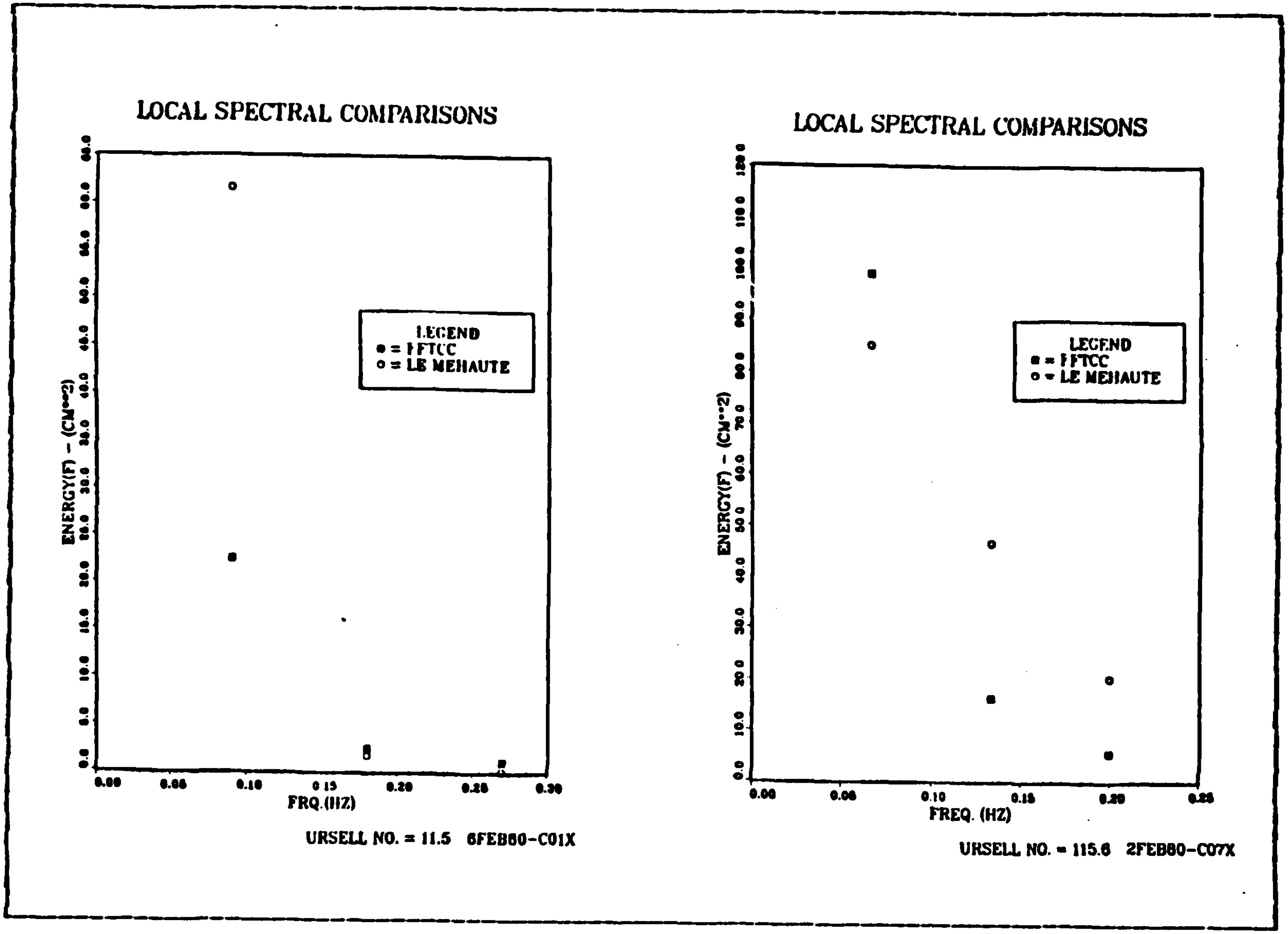

Figure 4 Local Spectral Comparisons for Small (left) and Large (right) Ursell Numbers.

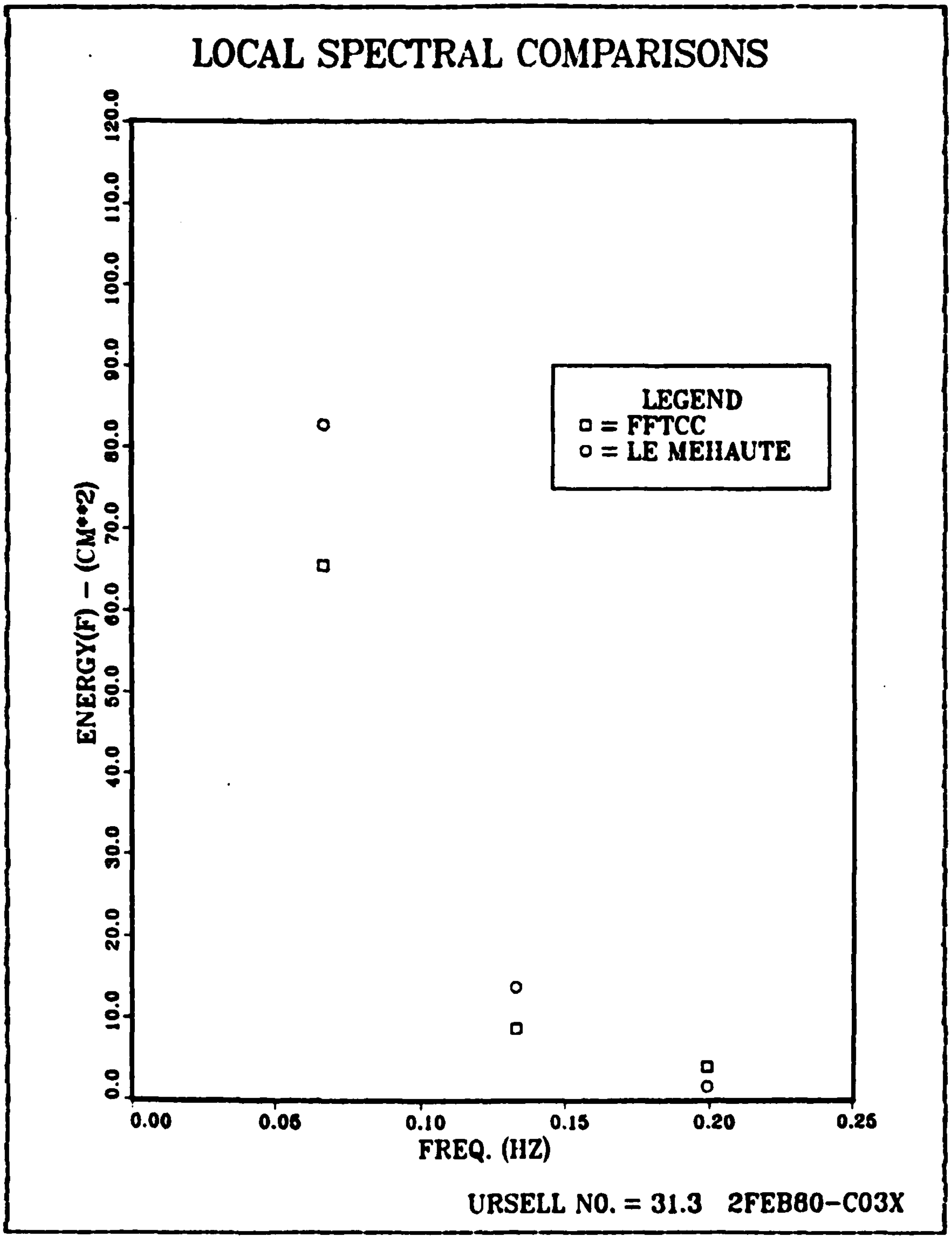

Figure 5 Local Spectral Comparisons for Intermediate Ursell Number.

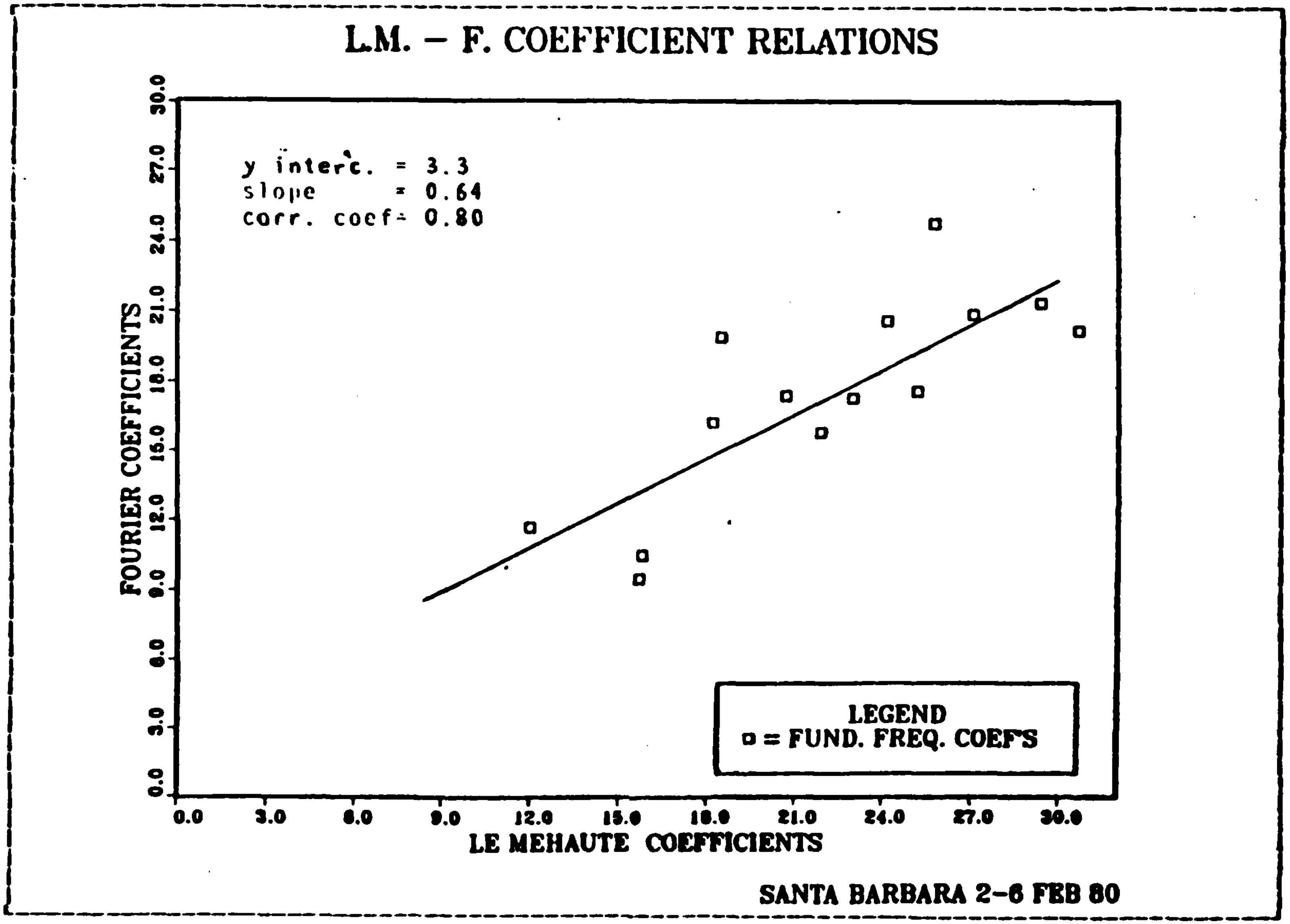

Figure 6 Fundamental Frequency Coefficients Correlation.

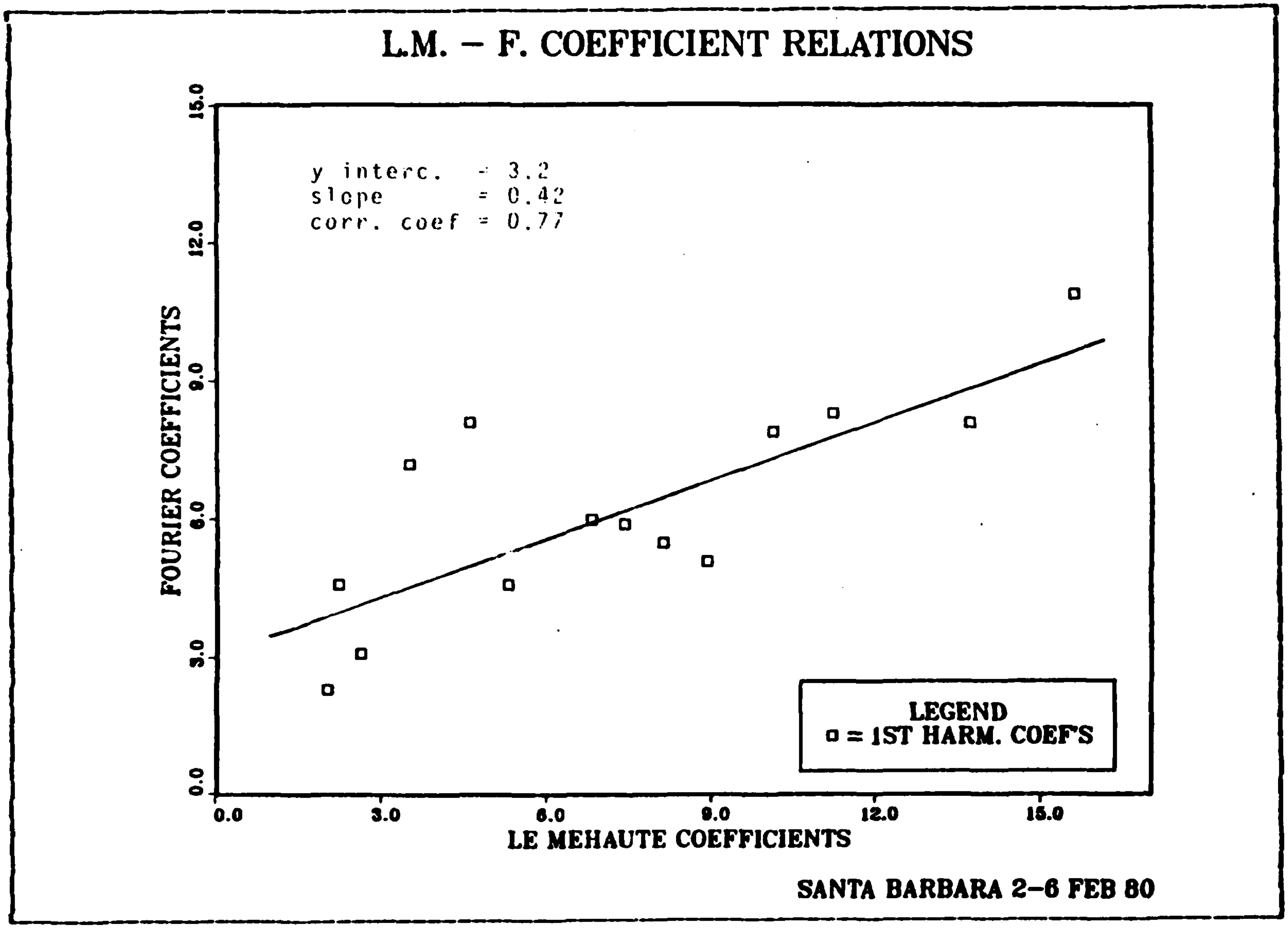

Figure 7 First Harmonic Coefficients Correlation.

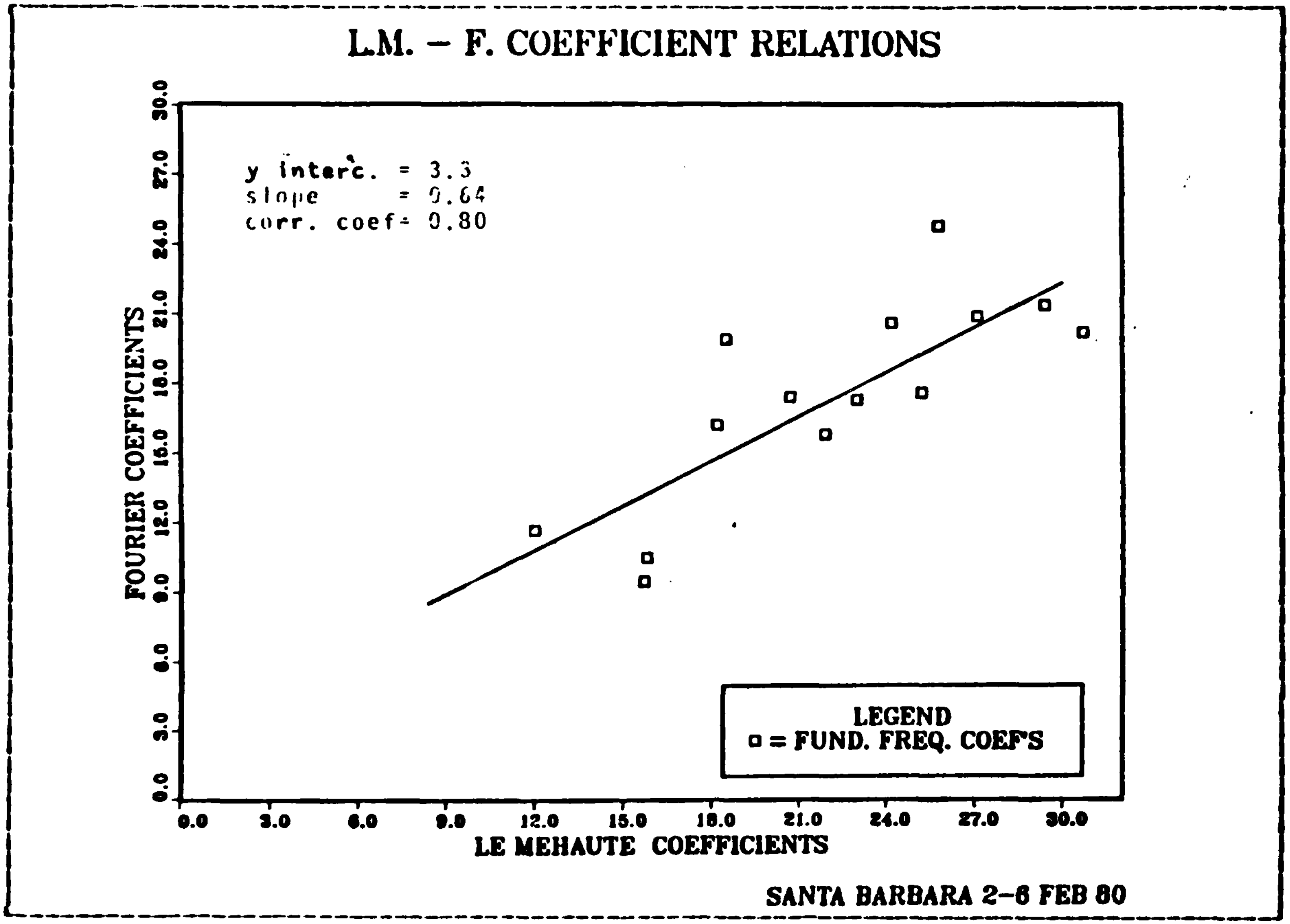

Figure 8 Second Harmonic Coefficients Correlation.

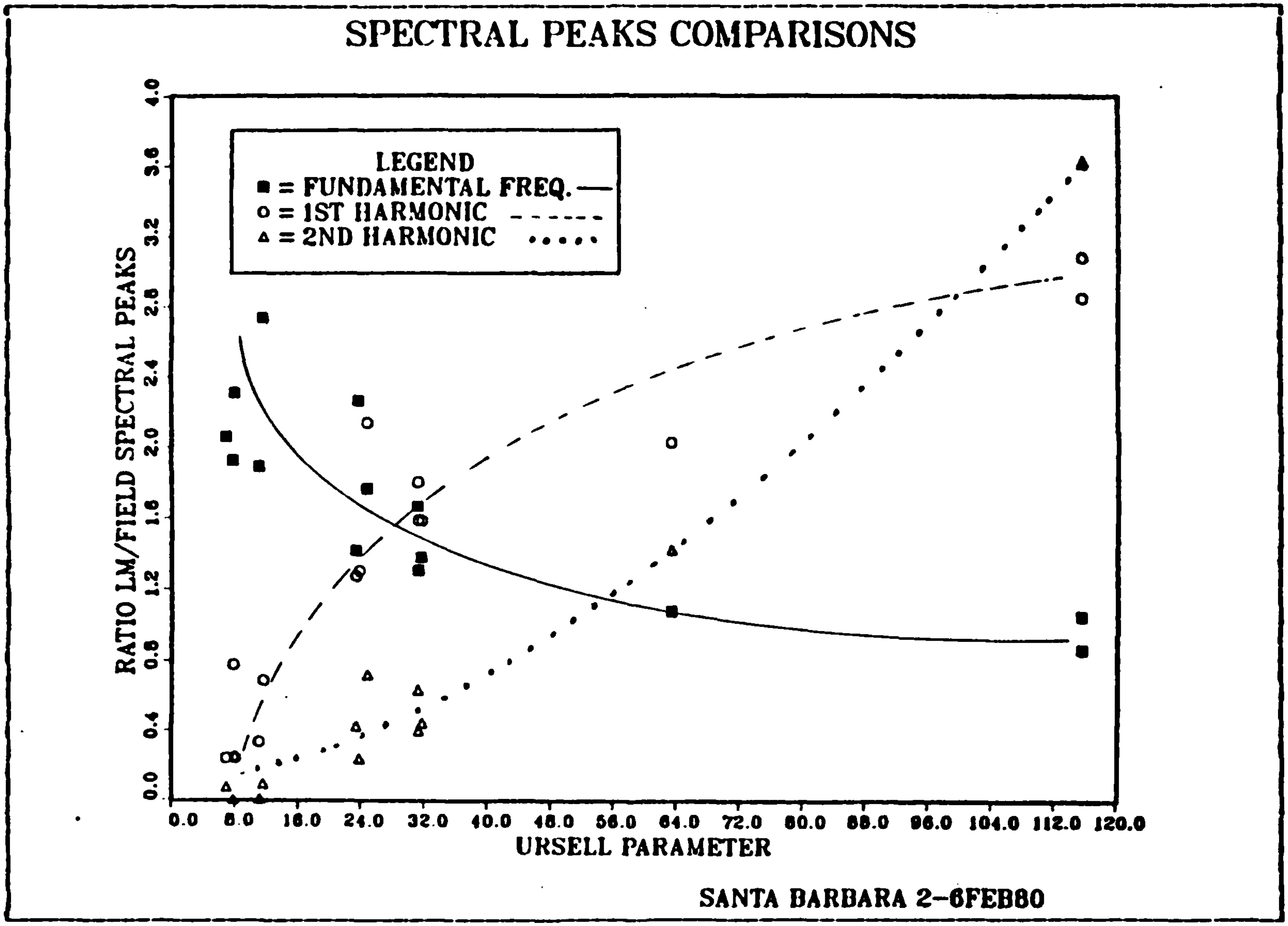

Figure 9 Spectral Peaks Comparisons against Ursell Number.

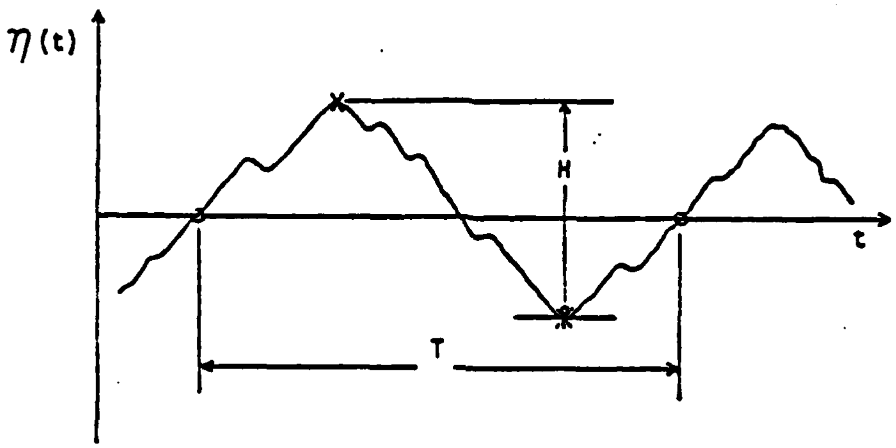

where X is a crest

* is a trough

0 is the zero-up crossing

Figure 10 Defining Waves using Zero-up Cross Method.

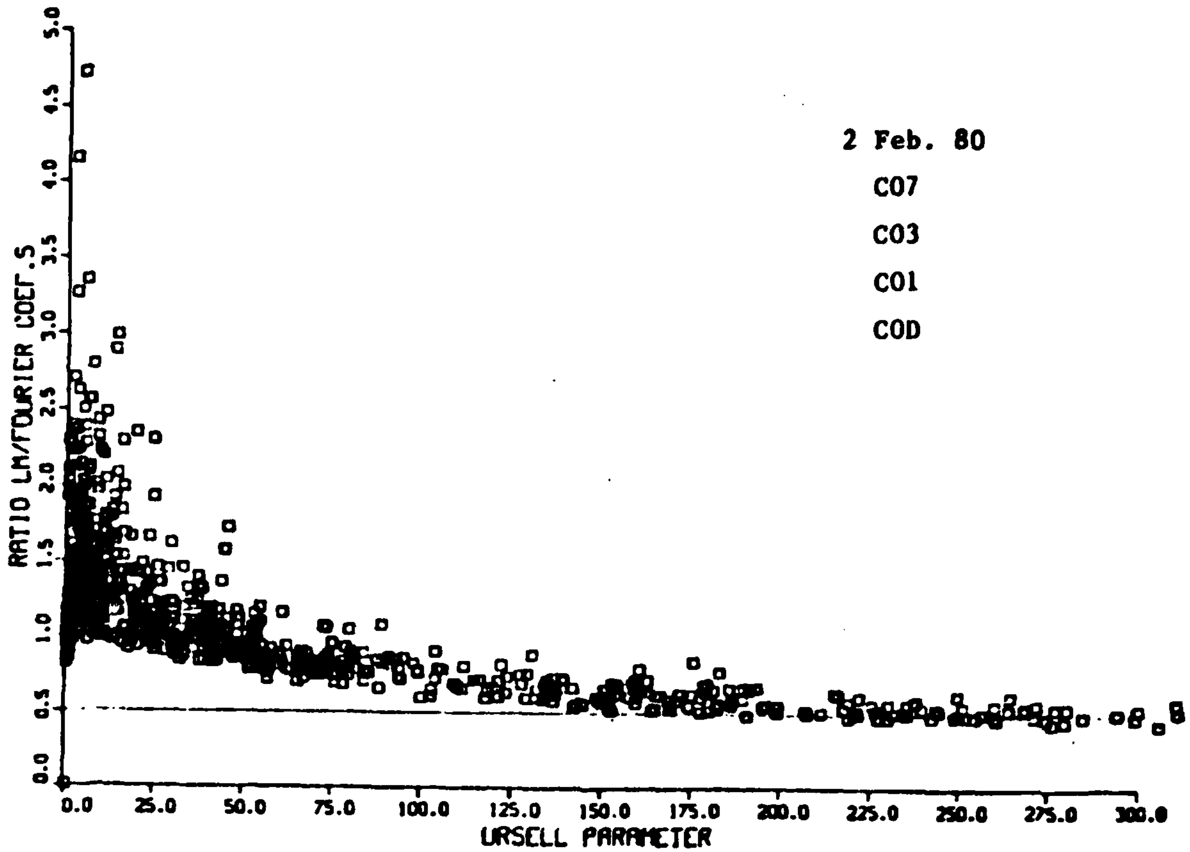

Figure 11 Coefficient Ratio at Fundamental Frequency against the Ursell Number.

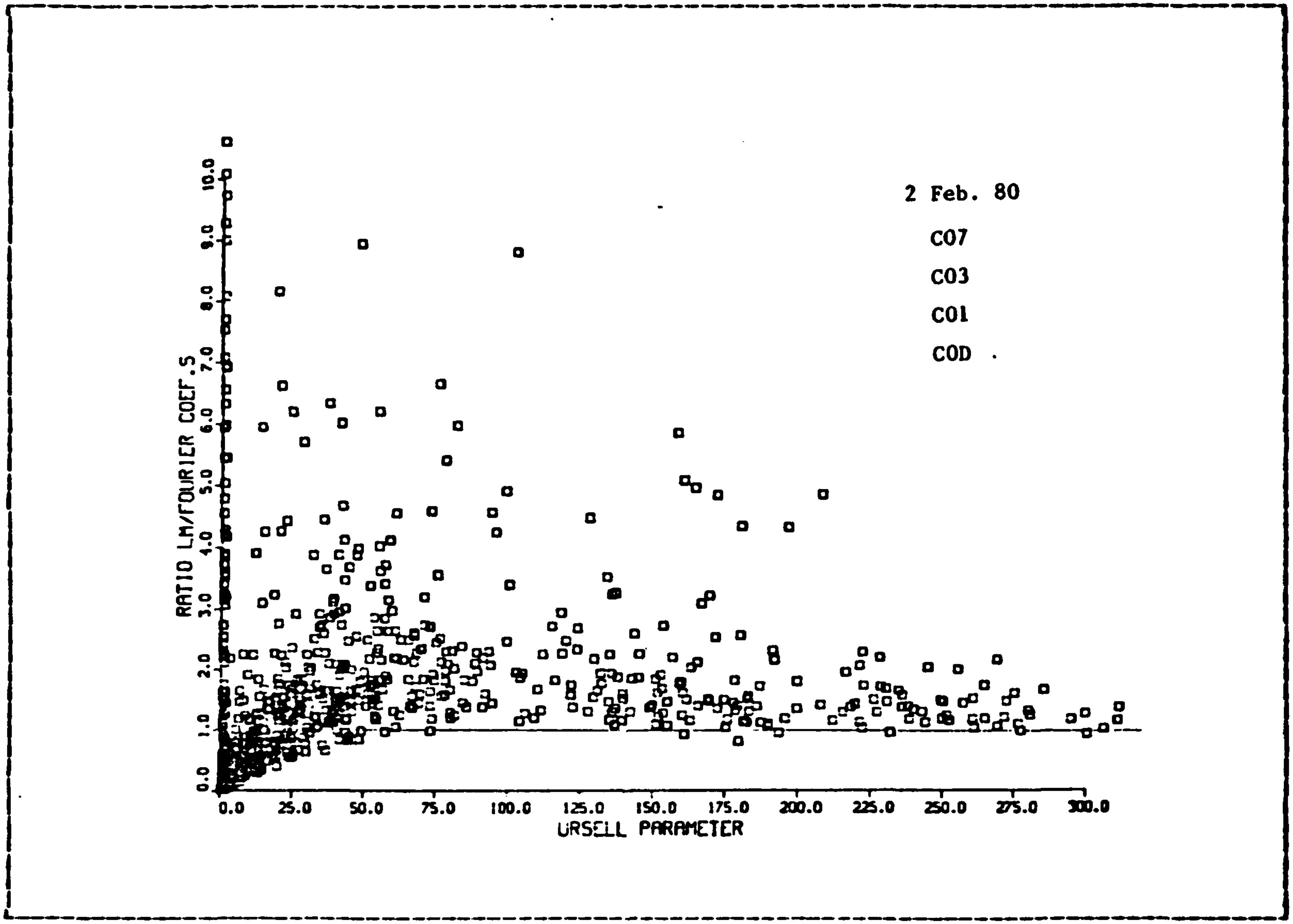

Figure 12 Coefficient Ratio at 1st Harmonic against the Ursell Number.

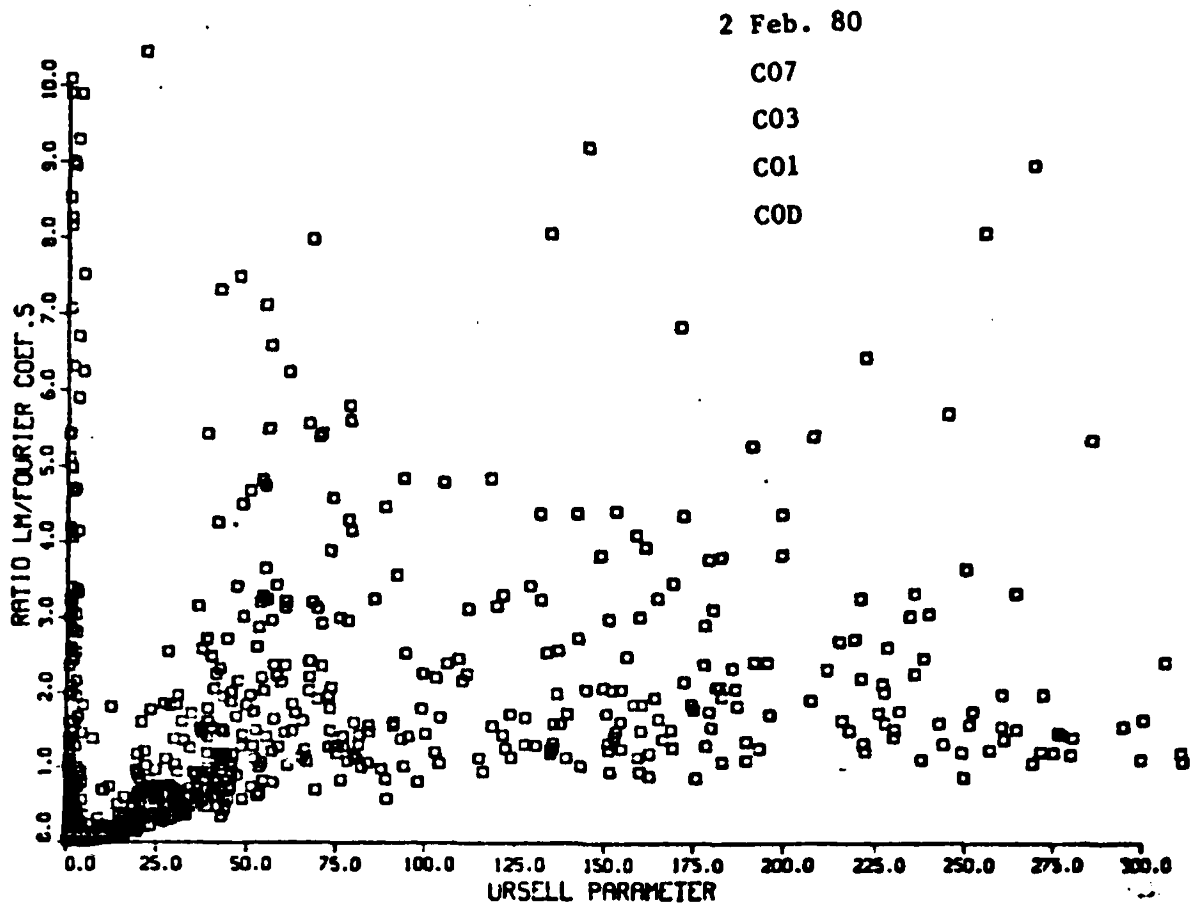

Figure 13 Coefficient Ratio at 2nd Harmonic against the Ursell Number.

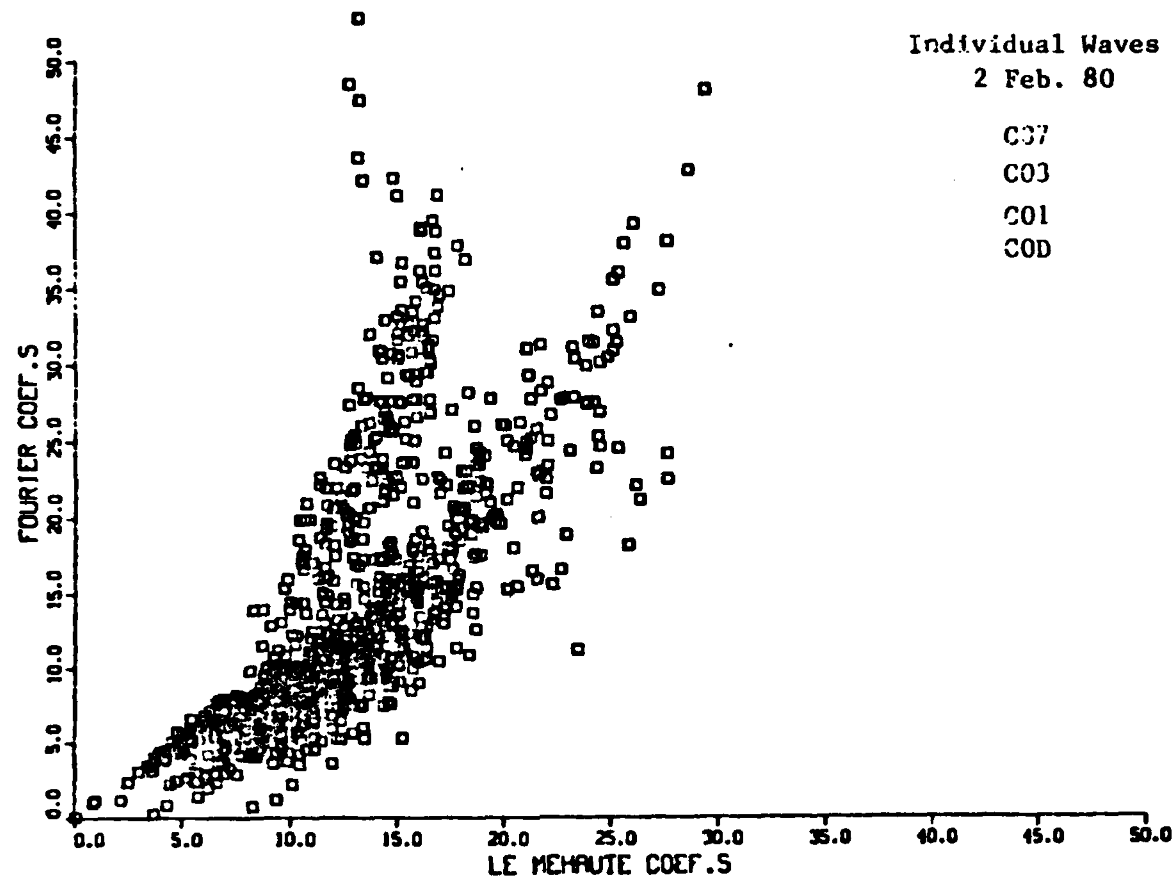

Figure 14 Correlation of the Coefficients at the Fundamental Frequency for all the Instruments.

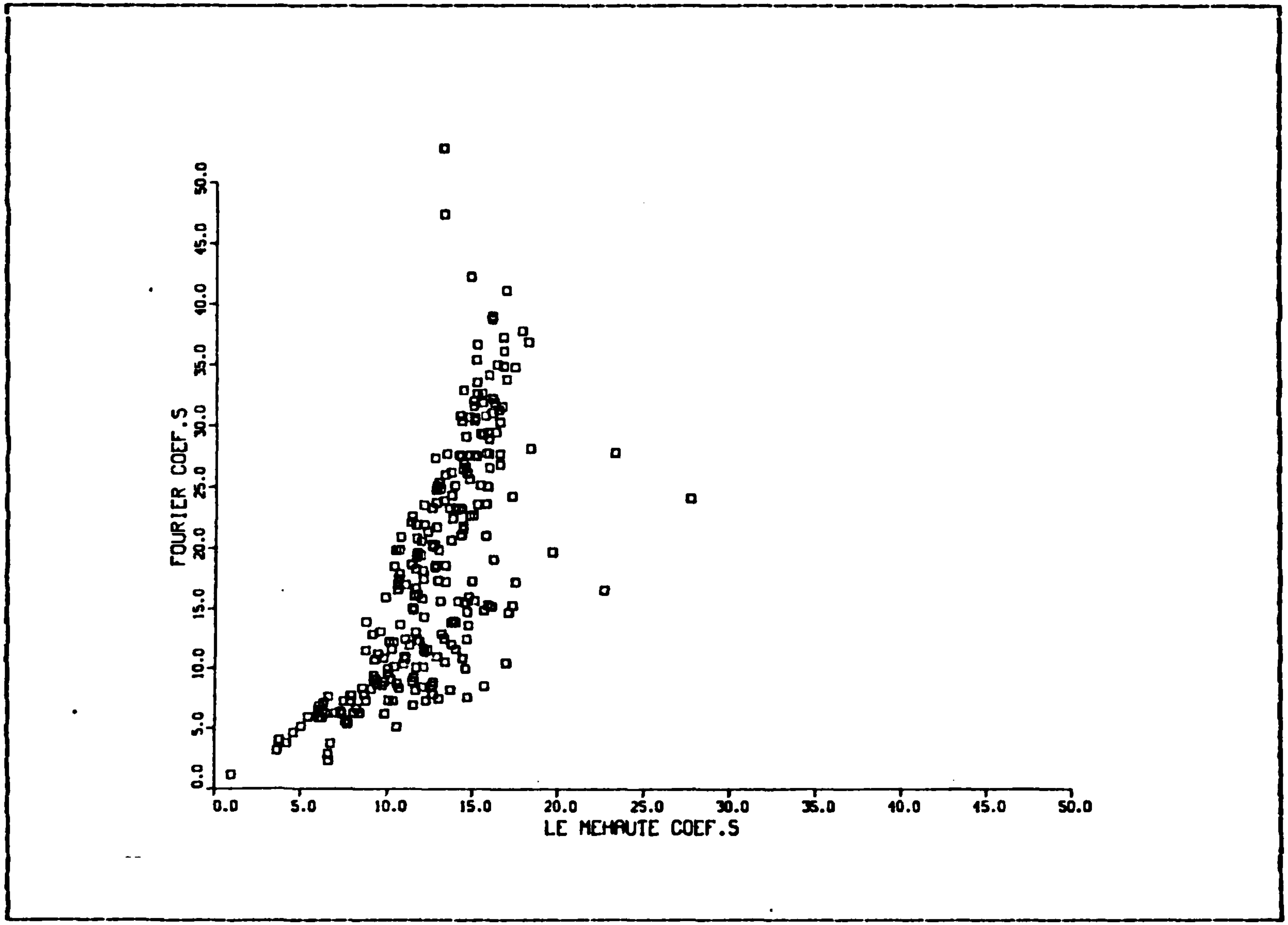

Figure 15 Correlation of the Fundamental Frequency Coefficients for the Current Meter C07 -2Feb.80.

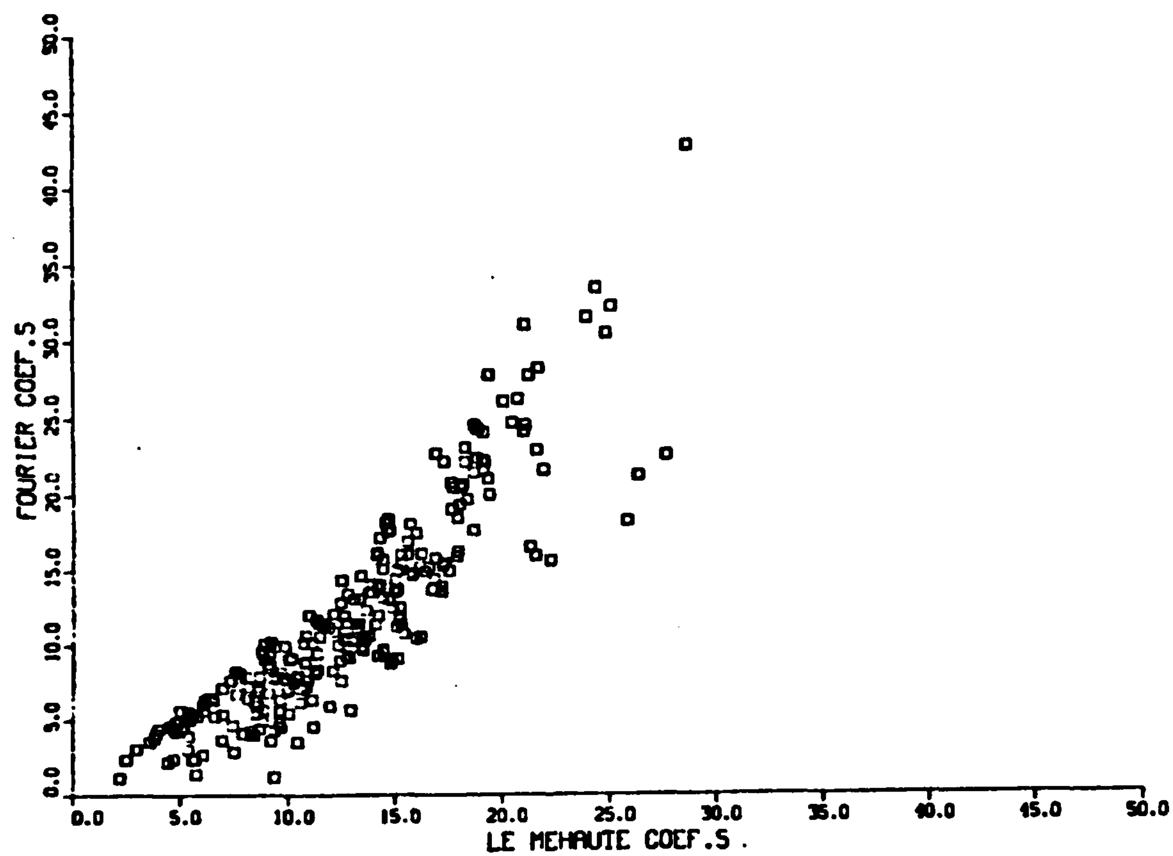

Figure 16 Correlation of the Fundamental Frequency Coefficients for the Current Meter C03 - 2Feb.80.

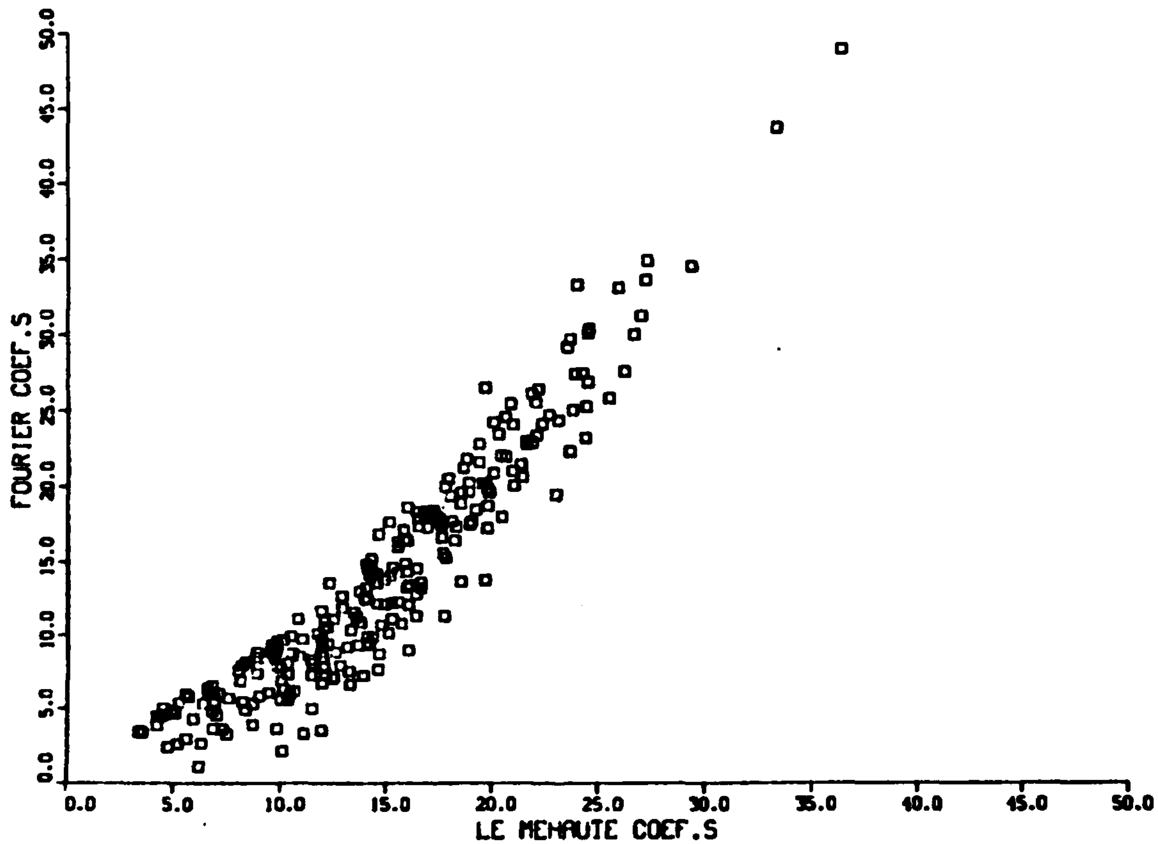

Figure 17 Correlation of the Fundamental Frequency Coefficients for the Current Meter C01 - 2Feb.80.

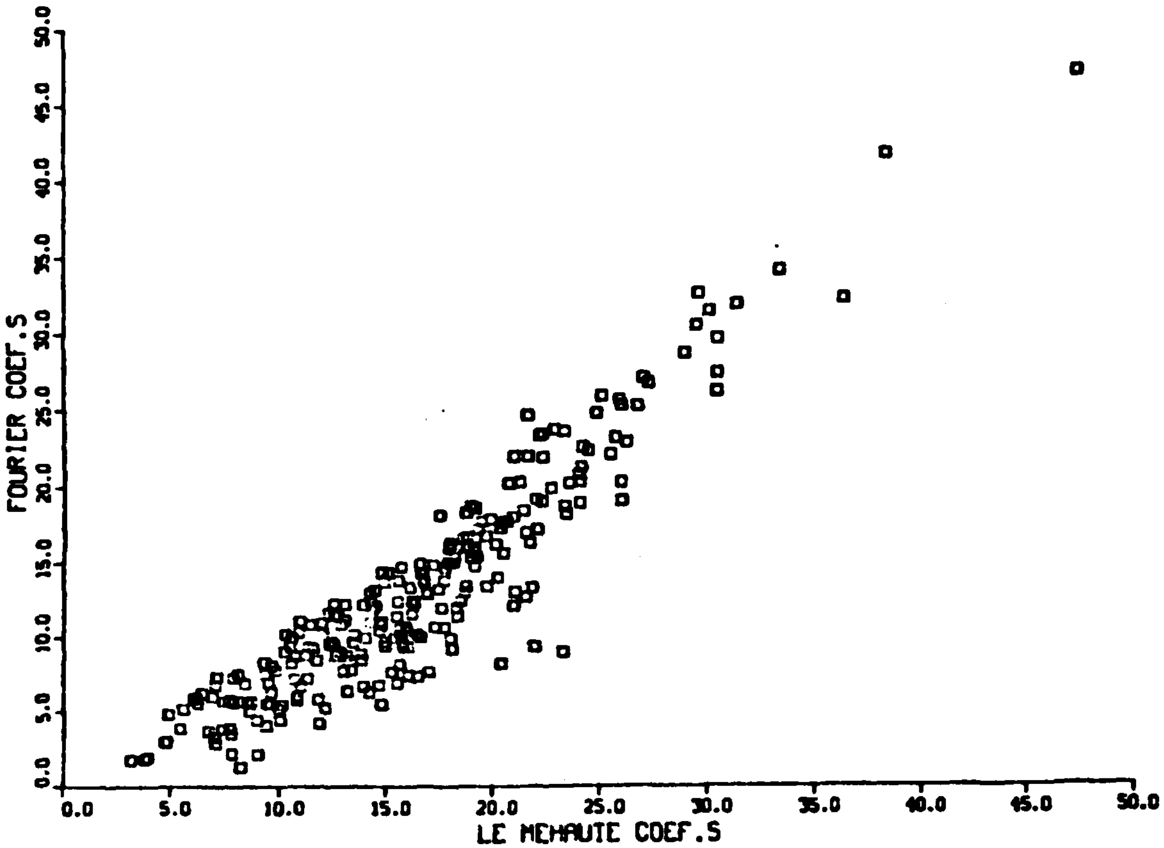

Figure 18 Correlation of the Fundamental Frequency Coefficients for the Current Meter COD - 2Feb.80.

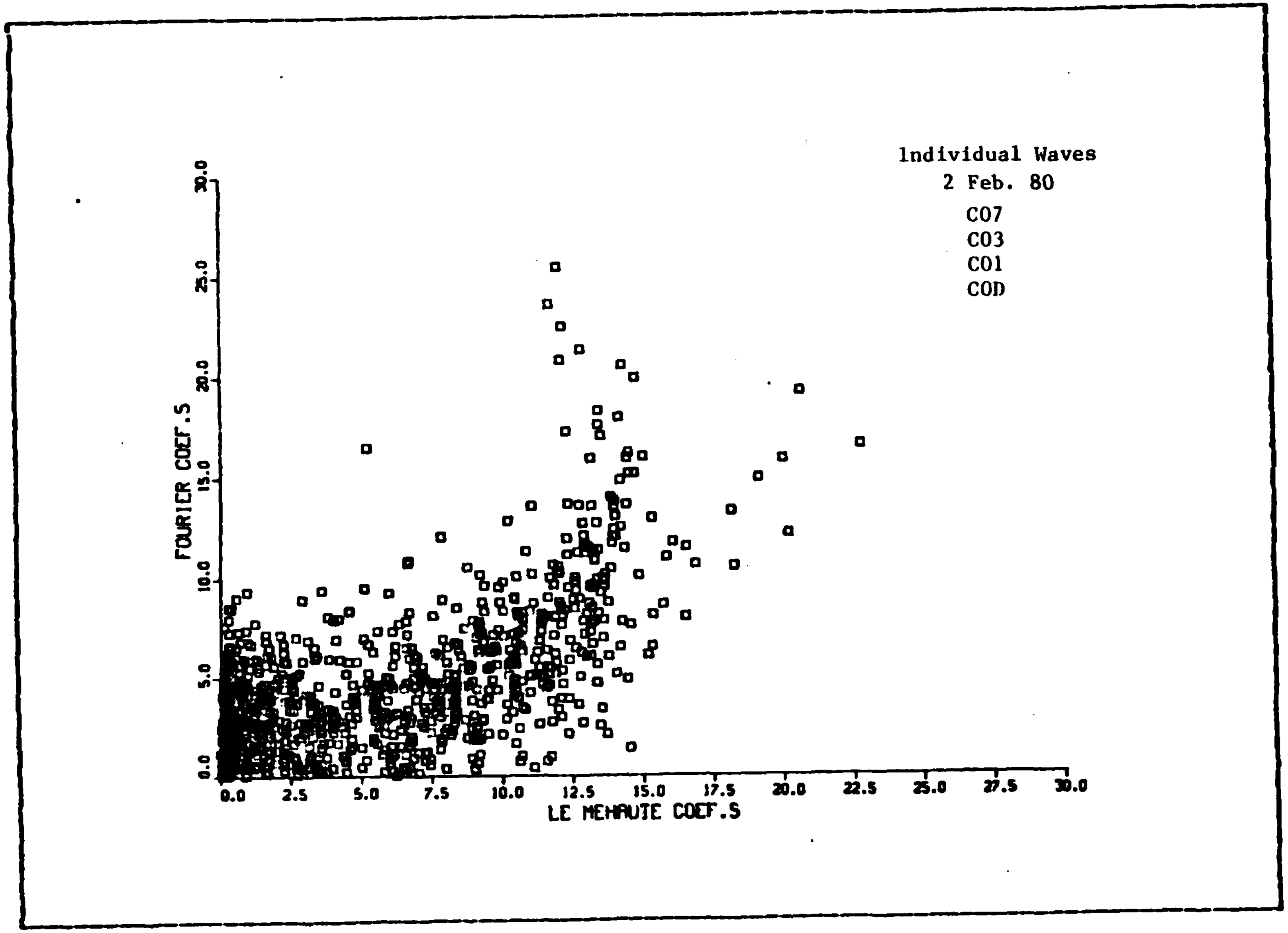

Figure 19 Correlation of the Coefficients at the 1st Harmonic for all the Instruments.

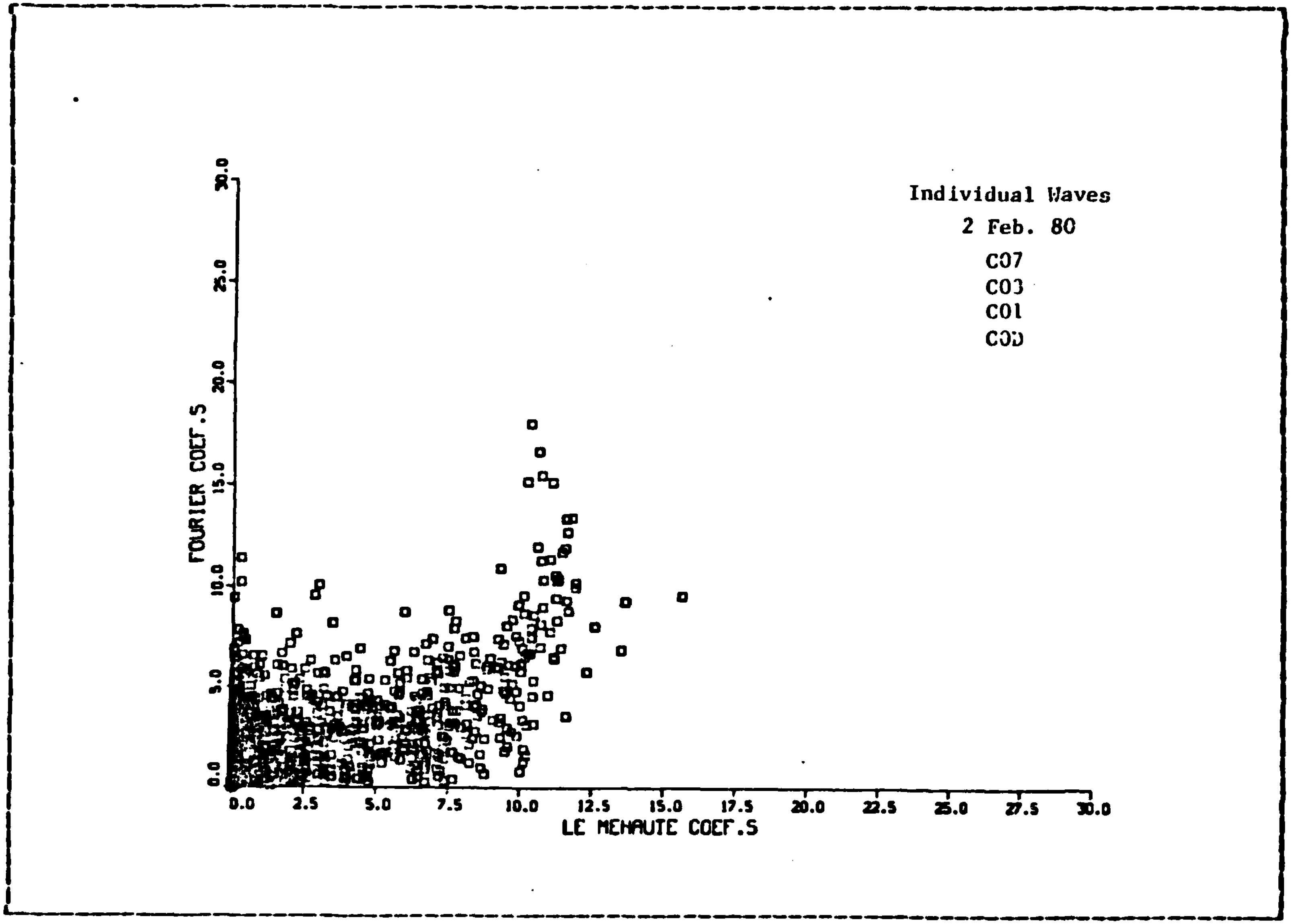

Figure 20 Correlation of the Coefficients at the 2nd Harmonic for all the Instruments.

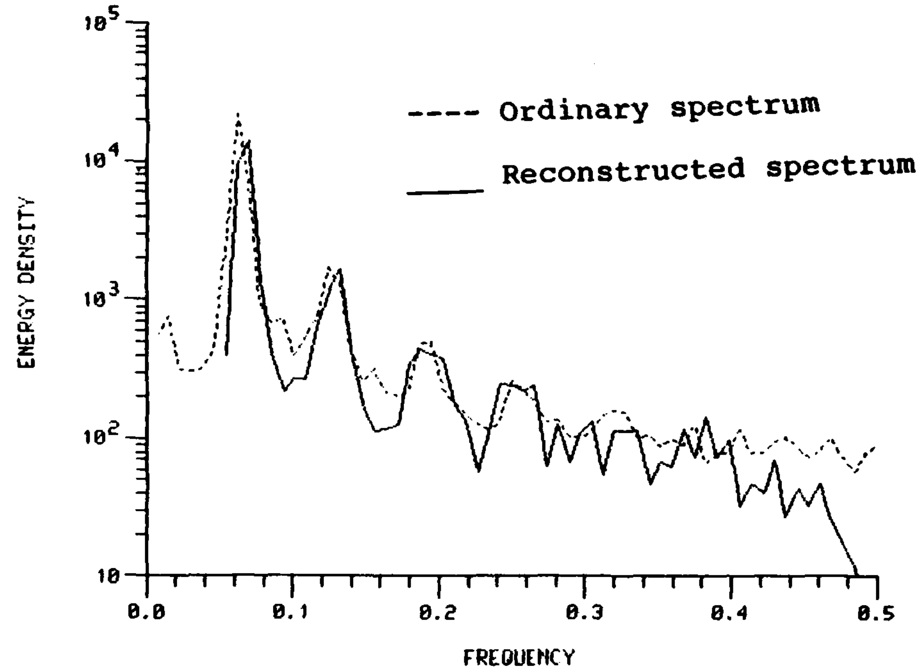

Figure 21 Comparison between Normal Spectrum and Nonlinear Reconstructed Spectrum.

BIBLIOGRAPHY

Airy, G. B., "Tides and Waves," Encyclopaedia Metropolitana, Art. 192, 1845, pp. 241-396.

Boussinesq, J., "Essai sur la Theorie des Eaux Courrantes," Institut de France, Academie des Sciences, Memoires presentes par Divers Savants, Vol. 23, 1877.

Chappelear, J.E., "Direct Numerical Calculation of Wave Properties," J. Geophysical Research, Vol. 66, No. 2, pp. 501-508, 1961.

Cokelet, E.D., "Steep Gravity Waves in Water of Arbitrary uniform Depth," Philos. Trans. Royal Society London A, Vol. 286, pp. 183-239, 1977.

Dean, R.G., "Stream Function Representation of Nonlinear Ocean Waves," J. Geophysical Research, Vol. 70, No. 18, pp. 4561-4572, 1965.

Dean, R.G., "Evaluation and Development of Water Wave Theories for Engineering Application," U.S. Army Corps of Engineers, CERC, Special Report No. 1, Nov., 1974.

Goda, Y., "A Unified Nonlinearity Parameter of Water Waves," Report of the Port and Habour Research Institute, Vol. 22, No. 3, Sept., 1983.

Korteweg, D. J., and de Vries, G., "On the change of the Form of Long Waves Advancing in a Rectangular Canal on a new Type of Long Stationary Waves," Philosophical Magazine, Ser. 5, London, Dublin and Edinburg, Vol. 39, 1895, p. 422.

Le Mehaute, B., Divoky, D., and Lin, Albert, "Shallow Water Waves. A Comparison of Theories and Experiments," Proceedings of Coastal Engineering Conference, London, England, 1968.

Le Mehaute, B., ASCE, M., Lu, C.-C., Ulmer, E.W., "Parameterized Solution to Nonlinear Wave Problem," Journal of Waterway, Port, Coastal and Ocean Engineering, Vol. 110, No. 3, August 1984.

Rienecker, M.M., and Fenton, J.D., "A Fourier Approximation Method for Steady Water Waves," J. of Fluid Mechanics, Vol. 104, pp. 119-137, 1981.

Schwartz, L.W., "Computer Extension and Analytic Continuation of Stokes Expansion for Gravity Waves," Journal of Fluid Mechanics, Vol. 62, 1974.

Stokes, G.G., "On the Theory of Oscillatory Waves," Cambridge Philosophical Society, Vol. 8, 1847, and Suppl. Scientific Papers.

Von Schwind, J.J., and Reid, R.O., "Characteristics of Gravity Waves of Permanent Form," J. of Geophysical Research, Vol. 77 No. 3, pp. 420-433, 1972.

INITIAL DISTRIBUTION LIST

		No. Copies
1.	Defense Technical Information Center Cameron Station Alexandria, VA 22304-6145	2
2.	Library, Code 0142 Naval Postgraduate School Monterey, CA 93943-5100	2
3.	Chairman (Code 68Mr) Department of Oceanography Naval Postgraduate School Monterey, CA 93943-5100	1
4.	Chairman (Code 63Rd) Department of Meteorology Naval Postgraduate School Monterey, CA 93943-5100	1
5.	Professor E.B. Thornton (Code 68Tr) Department of Oceanography Naval Postgraduate School Monterey, CA 93943-5100	3
6.	Professor C. S. Wu (Code 68Wu) Department of Oceanography Naval Postgraduate School Monterey, CA 93943-5100	1
7.	Jose Luis Branco Seabra de Melo Primeiro Tenente Rua Antonio Salvado Pires 3 R/C D.to 2130 Benavente, Portugal	3
8.	Director Naval Oceanography Division Naval Observatory 34th and Massachusetts Avenue NW Washington, DC 20390	1
9.	Commander Naval Oceanography Command NSTL Station Bay St. Louis, MS 39522	1
10.	Commanding Officer Naval Oceanographic Office NSTL Station Bay St. Louis, MS 39522	1
11.	Commanding Officer Fleet Numerical Oceanography Center Monterey, CA 93940	1
12.	Commanding Officer Naval Ocean Research and Development Activity NSTL Station Bay St. Louis, MS 39522	1

13. Commanding Officer 1
Naval Environmental Prediction
Research Facility
Monterey, CA 93940

14. Chairman, Oceanography Department 1
U. S. Naval Academy
Annapolis, MD 21402

15. Chief of Naval Research 1
800 N. Quincy Street
Arlington, VA 22217

16. Office of Naval Research (Code 420) 1
Naval Ocean Research and Development
Activity
800 N. Quincy Street
Arlington, VA 22217

17. Scientific Liaison Office 1
Office of Naval Research
Scripps Institution of Oceanography
La Jolla, CA 92037

18. Library 1
Scripps Institution of Oceanography
P. O. Box 2367
La Jolla, CA 92037

19. Library 1
Department of Oceanography
University of Washington
Seattle, WA 98105

20. Library 1
School of Oceanography
Oregon State University
Corvallis, OR 97331

21. Director 1
Instituto Hidrografico
Rua das Trinas, 49
Lisboa, Portugal

23. D. do Servico de Instrucao e Treino 1
Edificio de Marinha
Rua do Arsenal
1188 Lisboa, Portugal

24. Lab. Nacional Engenharia Civil 2
Avenida do Brasil
1700 Lisboa, Portugal